APPROVAL SHEET

Title of Thesis: Flexible Polyimide based 34-channel Electrode Arrays for
                     Mouse EEG Measurement

Name of Candidate: Fatima Nafisa Chowdhury
                     Master of Science, 2019 (to be conferred)

Thesis and Abstract Approved: _____
                                        Prof. Fow-Sen Choa, Ph. D.
                                               Professor
                                   Computer Science and Electrical Engineering
                                   University of Maryland, Baltimore Country

Date Approved: _____

ABSTRACT

Title of Document:	Flexible Polyimide based 34-channel Electrode Arrays for Mouse EEG Measurement
	Fatima Nafisa Chowdhury, MS, 2019 (to be conferred)
Directed By:	Professor Fow-Sen Choa Computer Science and Electrical Engineering

Electroencephalogram (EEG) recording is a widely used method to measure electrical activity in the brain. Unlike other noninvasive recording techniques, EEG technique allows sub-ms scale time resolution, which is essential to obtain causal relationship. In this work, we demonstrated a microfabrication process for developing a high-density polyimide-based rodent EEG recording cap. A 34-channel rodent electrode array with a total size of 11mmx8mm, individual electrode diameter 240µm and interconnect wire linewidth 35µm, was designed and fabricated. For the fabrication process, a silicon substrate was used and polyimide caps were fabricated. Gold deposition and lithography etching of 34-channel contact-electrodes, along with interconnects, was completed as next step. Fully developed EEG cap was then interfaced with a 34-channel female connector, which will then be connected to an ADC for acquisition and post-processing. This polyimide based EEG cap is biocompatible and flexible, and therefore, suitable for good contact with rodent skulls and non-invasive recording.

FLEXIBLE POLYIMIDE BASED 34-CHANNEL ELECTRODE ARRAYS FOR

MOUSE EEG MEASUREMENT

By

Fatima Nafisa Chowdhury

Thesis submitted to the Faculty of the Graduate School of the

University of Maryland, Baltimore County, in partial fulfillment

of the requirements for the degree of

Master of Science

2019

Dedication

*This thesis is dedicated
to my loving parents*

Acknowledgements

I would like to first thank my advisor Dr. Fow-Sen Choa for giving me the opportunity to work on this research project. In my research and writing, he has always helped me when I ran into any trouble and steered me in the right direction. The success and final outcome of this thesis would not be possible without his patience, immense knowledge, guidance and motivation.

I would like to express my gratitude to my committee members, Prof. Gary Carter, Prof. Li Yan and Prof. N. B. Singh for serving in my thesis committee and providing me valuable suggestions. I would like to thank my fellow lab mates, Deepa Gupta and Rachit Sood for the helpful discussions and encouraging words. Also I would like to thank Tim Buckheit for his timely support in clean room. I want to thank Dr. Mary K Lobo and Dr. Nam, from School of Medicine, University of Maryland, Baltimore whom we collaborated with for this research project.

I must express my profound gratitude to my parents and brothers Imran, Imtiaz for supporting and loving me unconditionally. I am thankful to and fortunate enough to get constant encouragement and support from my husband, Shahid, which always kept me going. Last but not the least, thanks to my toddler daughter Aneesha for being there in my tough times and relief my stresses with her adorable acts.

Table of Contents

List of Tables

List of Figures

(B–E) in BACE1–null mice. All eight of the recorded BACE1–null

mice showed at least some single spikes as shown in (A), while only

two of the wild-type mice showed occasional single spikes. The

pattern of discharge seen in (B) was recorded in one mouse with

spontaneous seizures. (C–E) Six of the eight BACE1–null mice

showed multiple spikes (C–D) or sustained spike-wave discharge

patterns (E). The scale bar is shown on the lower right [24].

Chapter 1: Introduction

Human brain is the main control center of its nervous system. It is perhaps one of the most complicated biological organs with an average of hundreds of billions of neurons. Brain is responsible for managing the information collection, generating the reaction on that information, if necessary and storing the information for future reference. Brain acquires information primarily through sensory system, responds to it through motor system and then selectively stores them in memory system. In this way, our brain is responsible for a large array of physical and mental activities, including perception, cognition, attention, emotion, memory and action. The main component of brain is neurons which has voltage gradient across its membrane. Ability to record electrical activity from brain tissues has been of significant interest to researchers who studies brain [1-3]. Neuron cell is an electrically excitable cell and serves as the primary structural and functional unit of brain tissues. Neurons communicate with each other through electrical signals, known as 'action potentials', 'nerve impulses' or 'spikes'. Reliable monitoring of these nerve impulses is critical to understand the activity pattern in a small or large neuronal network.

The junction between successive neurons are called 'synapse'. A person engaged in any kind of mental or physical activities is usually associated with having different regions of his/her brain stimulated during that time. This creates nerve impulses which passes through neurons via synapse and create neural network. Every neuron, by nature,

maintains a voltage gradient across its membrane, due to differences in sodium, potassium, chloride and calcium concentrations between inside and outside of cell body. Nerve impulses or action potentials are associated with a rapid change of these concentrations and therefore, it is often termed as 'electrical activity' in brain. These electrical activities can be measured and displayed as a wave form called brain wave or brain rhythm. Several scientific techniques such as Electroencephalography (EEG), Electro-corticography (ECoG), Magnetic Resonance Imaging (MRI), functional Magnetic Resonance Imaging (fMRI), Positron Emission Tomography (PET) And Single Photo Emission Computed Tomography (SPECT) have been demonstrated to be very useful tool to monitor these brain activities [16].

Electroencephalogram, commonly known as EEG, is a widely used method for recording electrical activity in brain [4, 20]. EEG recording in human brain yields useful spatio-temporal information about brain activities. However, human brain is a significantly complex structure that consists billions of nerve cells and several hundred trillion of connections between them. To understand the brain activity, researchers generally aim to focus on a very specific section of the brain and that requires recording from a much smaller and simpler network of neurons. Rodent animal models are usually chosen for most of these studies since their brains have a simpler architecture than a human brain while it is complex enough to be comparable to activity patterns in a human brain. However, Unlike EEGs for human brain, EEG electrodes for rodent brain need to be significantly smaller in size and this brings few challenges in making reliable EEG electrodes at that scale.

Over the years, there has been a variety of EEG electrodes developed from microneedle-based to pin-based electrodes to record brain signals [1-3, 5-6]. Polyimide based microelectrode is a relatively new approach and it enables the recording of activity at very high spatial and temporal resolution. Some early pioneer works in this direction has investigated this approach and opened the door to new possibilities [7-10]. These reported polyimide-based electrodes have shown the potential for recording activity with high resolution. Polyimide-based electrodes brings the mechanical flexibility in the electrode positioning while it is also biocompatible to be used directly or near to brain surface [11-12].

In this work, we have focused on the design and development of a flexible substrate polyimide-based 34-channel mouse EEG cap. As a follow up of our previous works on Kapton film based 8-channel electrode, as shown in Figure 1.1, increasing the number of electrodes was the next logical step [13-15]. This work was focused on the design and development of 34-channel electrode. In our previous work with 8-channel mouse EEG, we were able to record mouse EEG signals and various cardiac artifacts. To accomplish better accuracy for 2D to 3D sLORETA conversions and to employ independent component analysis (ICA), we need more channels [14-15].
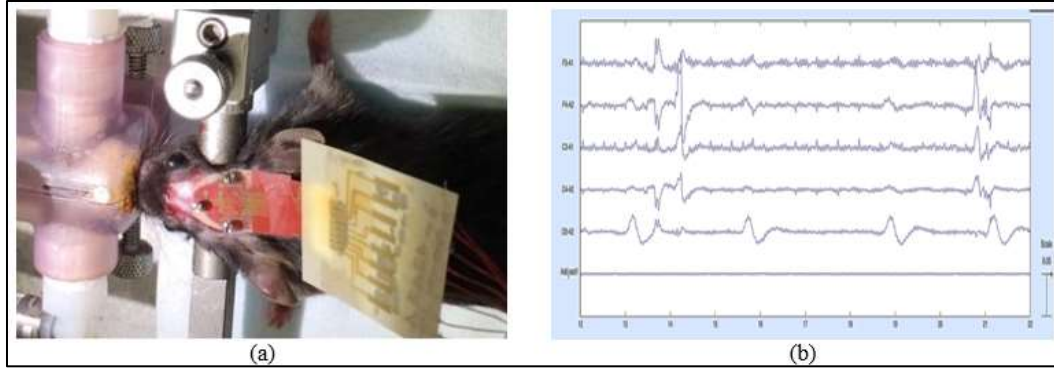
Figure 1.1. Our previous work on mouse EEG using 8-channel electrode. (a) 8-channel electrode device installed on mouse brain, (b) recorded EEG signal from different channels [13].

Apart from increasing the number of electrodes to four times, the fabrication process was significantly different in this work. One of the goals of this work was to develop an EEG cap which is flexible and biocompatible, so that we can do long-term recording from the same region of interest in brain while keeping the recording site minimally impacted. Increasing the number of electrodes offers the opportunity to have better spatial resolution and therefore, allows to move one step closer to the resolution that is relevant to study the brain activity at the neuronal level. With increased number of electrodes for a given surface area, this also brings challenges, such as, risk of overlapping electrode lines, signal crosstalk between adjacent electrodes and complexity in interfacing of this higher number of electrodes to the next section through connection pad.

This thesis is organized in 6 chapters. Chapter 1, as described above, introduced the research area and motivation behind this work. Chapter 2 provides a background review. It discusses mouse brain anatomy, history of EEG and a brief literature review

of mouse EEG techniques and developments over the recent years. Chapter 3 focuses on the design aspect of this work, elaborately describes the design considerations and challenges in material selection. Chapter 4 provides a comprehensive overview of the fabrication steps that were followed to implement the design and eventually to build the 34-channel, flexible and biocompatible electrode. Chapter 5 briefly explains the procedures involved in testing the device and then interfacing it to external connector. Chapter 6 summarizes the outcome of this work and later, outlines the future work that are to follow to complete the system level integration of this developed electrode and therefore, to use this for mouse EEG application.

Chapter 2: Background Review

In this chapter, a background of the research work is presented. First section of this chapter reviews the mouse brain structures and its major components. Then an overview of EEG and its history is provided. The last section of this chapter highlights the previous works that have been accomplished along the same or similar direction of this research.

2.1 Basic Structure of Mouse Brain

In order to design mouse EEG device a basic understanding of different part of the mouse brain is important. A good understanding of physical dimensions of mouse brain helps to define the size of the device and to design electrode in such a way that all the regions of interest will be covered. The mouse brain is primarily made of four different parts, which are Frontal Association Cortex, Somatosensory Cortex, Auditory Cortex and Visual Cortex.

2.1.1 Motor and Frontal Association Cortex

Most of the conscious thoughts and decisions are made in this region. Frontal association cortex is known to be responsible for reasoning, planning, parts of speech, emotions and problem solving. Frontal cortex contains motor areas that controls voluntary movements of all of our limbs and eyes. This lobe also contains most of the dopamine-sensitive neurons. This is important to note since the dopamine system is

responsible for many cognitive processing involving reward, attention, short-term memory, planning and motivation. Unlike human, mice are not known to have the ability to do abstract thinking and most of cognitive functions, so their frontal association cortex is relatively small in proportion [16].

2.1.2 Somatosensory Cortex

Somatosensory cortex is a subset of the sensory system that deals with the conscious perception of touch, pressure, pain, temperature, position, movement, and vibration, which arise from the muscles, joints, skin, etc. It is a set of modules of the neocortex responsible for processing sensations of touch. Having an architecture of neocortical areas used for processing sensory information, mouse neocortex has become a classical model system to researchers due to its experimental accessibility [16]. For example, the whisker system is an important sensory organ with broad neural representations in the brain of the mouse. Whiskers are heavily used by mouse to probe the sensory environment and due to high volume of activity in that area, they have a relatively large somatosensory area than other parts of the brain.
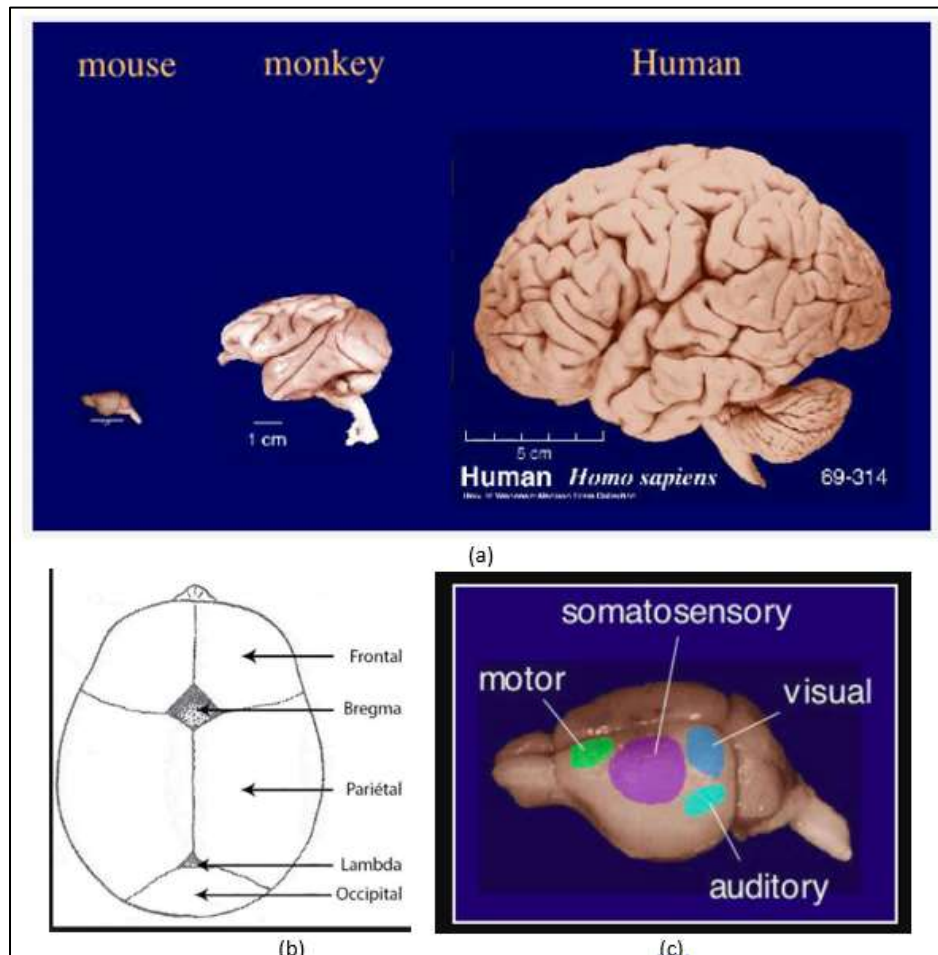
Figure 2.1 (a) Comparison of mouse, monkey and human brains; (b) and (c) Major regions of mouse

brain [17, 18]

2.1.3 Auditory Cortex

External auditory signals are recognized and processed in the temporal lobe cortex of

mouse brain. Temporal lobe is associated with processing sensory inputs relating to

visual memories, language and emotional association. Temporal cortex is known to be

also responsible for long-term memory formation and storage [16]. Left temporal

cortex, that contains Broca's and Wernicke's areas, is responsible for language

8

comprehension, processing and production. Deep temporal structures include the hippocampus, which is one of the key structures that contributes to navigation, biographic memory encoding and retrieval. Damage to these regions can cause significant deficits in reading or talking.

2.1.4 Visual Cortex

Visual cortex is located in a brain region known as Occipital lobe. It is located under the rearmost portion of the skull. Occipital lobe is called the visual processing center of the brain and it includes low-level visuospatial processing such as orientation and spatial frequency, color differentiation and motion perception [16]. Lesion in the Occipital lobe are usually associated with visual hallucinations, color or movement agnosia and can be severe enough to cause blindness.

2.2 Electroencephalography (EEG)

This section provides a basic overview of electroencephalogram (EEG) and its history.

2.2.1 Definition of EEG

Electroencephalography (EEG) is a technique for the non-invasive recording and characterization of electrical potential at different positions of scalp and therefore, a method to record brain activity. EEG is a graphic plot of voltage with time. Scalp electric potential distributions represents brain's internal electric currents associated with active neurons and can be measured simultaneously at discrete recording sites on

the scalp surface over a period of time. Most conscious brain activity is generated within the cerebral cortex, which is the outer surface of brain comprised of approximately ten billion neurons and have well localized active regions. Through synchronous synaptic stimulation of a very large number of neurons, they align themselves orthogonally to the cortical surface. When a large group of such neurons all depolarize or hyperpolarize together, they result in a dipolar current signal oriented perpendicular to the surface. It is the propagation of this current that we measure using EEG [19].

EEG has a high temporal resolution and therefore, can capture the physiological changes underlying the cognitive processes much better than other brain imaging techniques (such as MRI or PET scanners). EEG voltage is typically around 5-75 µV. Most cognitive processes occur within tens to hundreds of milliseconds – much faster than a blink of an eye. In addition, the events triggering cognitive processes occur in time sequences that span hundreds of milliseconds to a few seconds.

2.2.2 Basic Essentials and Developments of EEG

Systems used to acquire and record EEG signals usually have two functionally distinct part: the amplifier used to increase the voltage of the input signal and the output device used to display the amplified signal. Adrian and Matthews (1934) first recorded EEG. During 1930s, Hans Berger, a German Neuro-psychiatrist, used large pad electrodes placed on the forehead and on the rear of the head but later decided to employ localized recording electrodes of diameter of 5-7mm. Some researchers used flattened pallet of

solders, other used gold or silver disks. Unlike now, at that time, there were not many choices of amplifying unit and recording equipment.

Human studies seeks physiological and pathological correlates of EEG. In pathological correlate it soon became evident that clinical patient with neurological disorders such as epilepsy in its several forms, brain tumors, brain trauma, and other brain damaging factors cause the brain to produce striking electrical patterns in the EEG very different from those characteristics of the normal brain. Physiological studies were concerned with blood sugar level, acid-base balance, metabolism, drugs and anesthetics and fatigue. And psychologically oriented investigation of the EEG in an effort to determine experimentally in what way EEG correlates with sensory experience, perception, learning, emotion, motivation, and other factors.

While single EEG scalp electrodes provided estimates of synaptic sources averaged over tissue masses containing up to 1 billion neurons, Kornmuller recognized the importance of recording from a greater number of electrodes with the introduction of microelectrode technique in the early 1950s EEG branched out into the world of single neurons. It was made out of tungsten with tips of 1-3 micrometer in diameter; glass electrodes filled with electrolytes such as KCl but their high impedance values (1-60Mohm) made them unsuitable. Extracellular and Invasive intracellular EEG technology progressed rapidly after then until year 2000.

In most recent years, EEG, as an imaging method, has become relatively less expensive and portable. The ease of combination with other imaging tools has also enhanced and recording also has changed from analog to digital recordings. Large scale multiple sensor together with additional analytical capabilities will be the next steps in EEG research. High density EEG system provide very good spatial resolution. Neuronal activities in specific brain areas can be reconstructed with millisecond resolution by applying source analysis method [21].

2.2.3 Difference between Human Brain EEG and Mouse Brain EEG

The main similarity between human EEG and mouse EEG is that the end goal is same – recording activity-induced electric potentials in brain using a set of spatially distributed electrodes. One of the main differences is the size – human brain is several orders of magnitude bigger than a mouse brain, although they do share a similar brain-body mass ratio, as shown in Figure 2.2 [22].
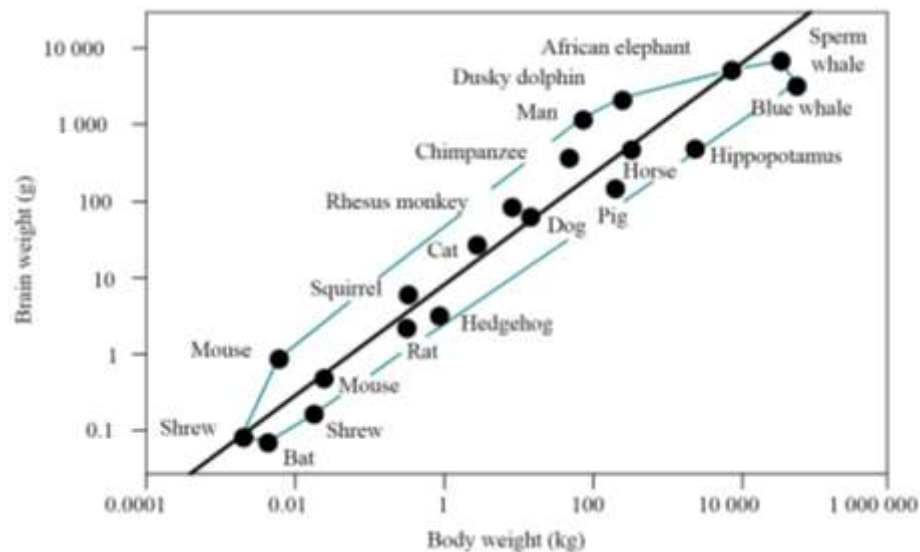

Figure 2.2 Brain-body mass ratio relationship for different mammals [22]

Another difference is the complexity in structure and function between two brains. Human brain has more complex architecture, bigger cortical regions and larger number of synaptic connections that allow for more advanced cognitive processing and large scale memory management. With respect to EEG, mouse brain is a very useful model to understand human brain since investigators can focus their research in a simpler model first and then can relate the findings with human brain. Below are two examples (Figures 2.3 and 2.4) of EEG recordings in human and mouse brain during experiencing seizure or epileptic activity [23, 24].
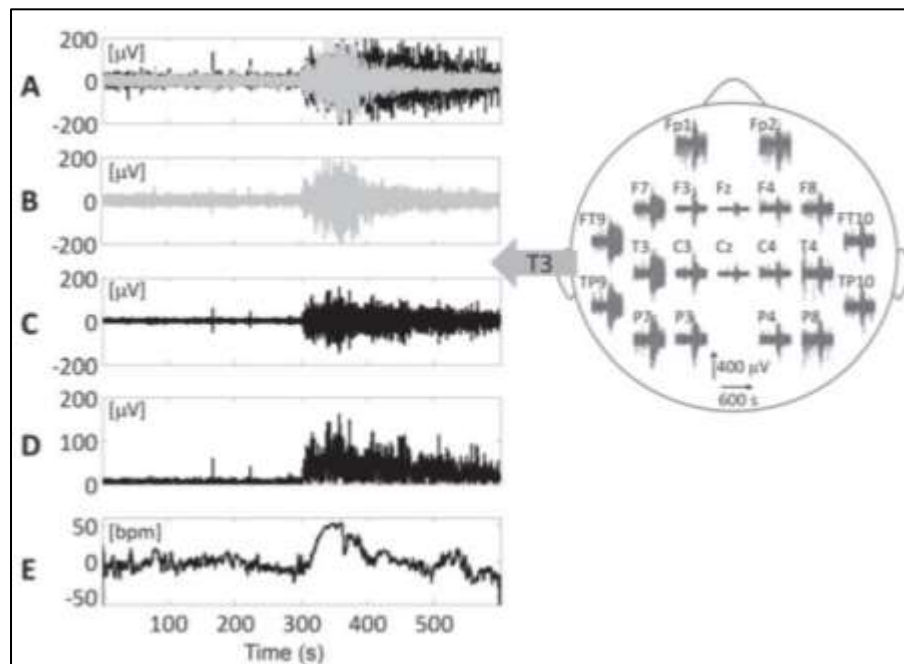
Figure 2.3   Examples for recorded and processed EEG signals from human brain (a child). (A) The EEG at electrode T3 with the overlay (gray) of average reference activity, (B) average reference activity, (C) activity of the δ sub-band 1.5 – 4 Hz, (D) envelope of the δ sub-band and (E) HRV (linear trend was subtracted), all given for one child. Additionally, overview of recorded EEG at all electrode positions is depicted for the same child [23].
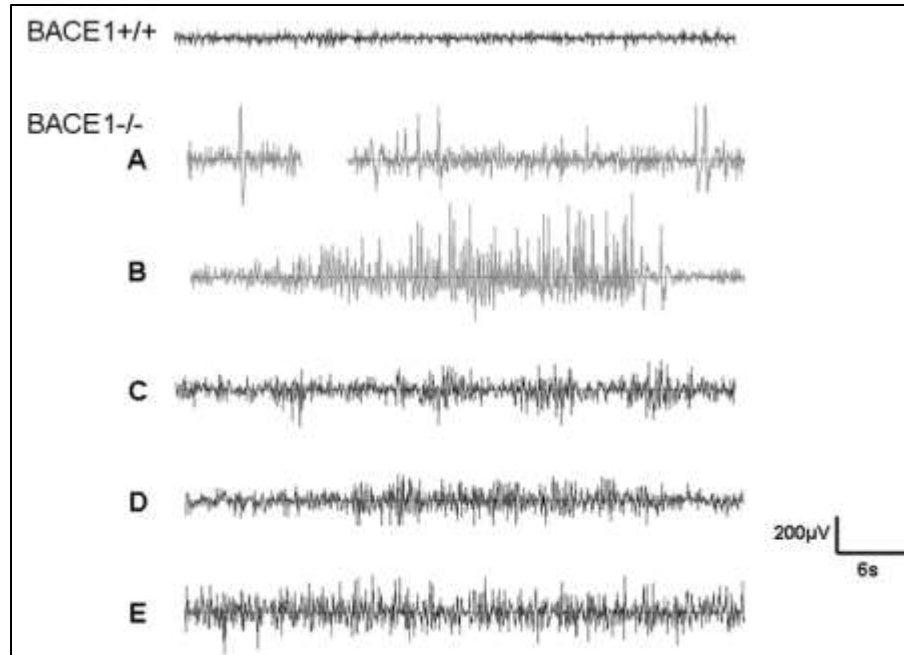
13

Figure 2.4 Spontaneous epileptic seizures in BACE1–null mice Representative EEG recordings shown from both BACE1+/+ and BACE1-/- mice. Spike amplitude (µV in Y–axis) is plotted as a function of recorded time course (s in X–axis). Variable patterns of spiking can be seen, ranging from single or multiple spikes (A) to spike-wave discharges (B–E) in BACE1–null mice. All eight of the recorded BACE1–null mice showed at least some single spikes as shown in (A), while only two of the wild-type mice showed occasional single spikes. The pattern of discharge seen in (B) was recorded in one mouse with spontaneous seizures. (C–E) Six of the eight BACE1–null mice showed multiple spikes (C–D) or sustained spike-wave discharge patterns (E). The scale bar is shown on the lower right [24].

2.3 Literature Review of Mouse EEG

The research in early 1930s had mainly two directions, one of them was animal studies seeking to identify source and nature of EEG and the other one was human studies seeking physiological and pathological correlates of EEG. The first animal EEGs were done under anesthesia by Fischer (1932) and Kornmüler (1932) and Bartley and Bishop in Germany (1932, 1933) and Travis and Dorsey (1932) in United States [16, 20]. Electroencephalography from genetically manipulated rodents (mostly mice) yields primary information to comprehend neurobiological phenomena. In recent years,

14

remarkable achievements have been reported in brain development, brain disease analysis, and pharmacological effects for neuroscience, translational research and neural engineering, through EEG recordings from mice [25-27]. This sections provides an overview of different types of EEG electrodes that have been used in earlier studies.

2.3.1 Intracellular Electrode

Intracellular electrode was fundamental to understanding the single cell neurophysiology, but it is difficult to scale and is damaging to cell.

2.3.1.1 Screw Electrode and Wire Electrode

Stainless screws often serve as recording electrodes, which require either drilling holes into the skull to insert screws or affixing screws to the surface of the skull with adhesive. Drilling holes large enough to insert screws can be invasive and damaging to brain tissue, using adhesives may interfere with conductance and result in a poor signal, and soldering screws to wire leads results in fragile connections. Also this invasive method has major risk of infection and also hemorrhage to occur. Wire electrodes are minimally invasive than screw electrodes. Research shows that the quality of recording from these rigid electrodes degrades eventually in addition to tissue damage.
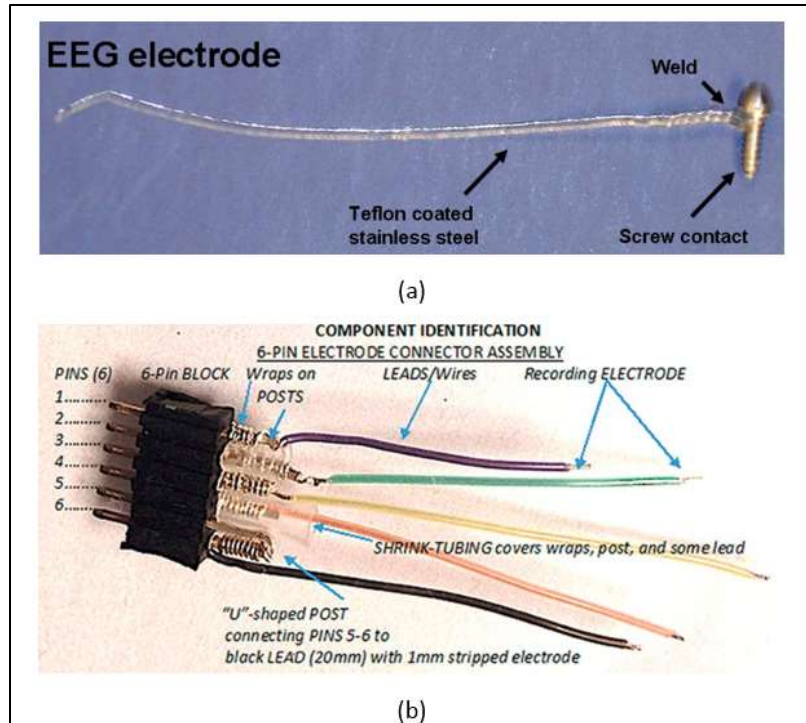
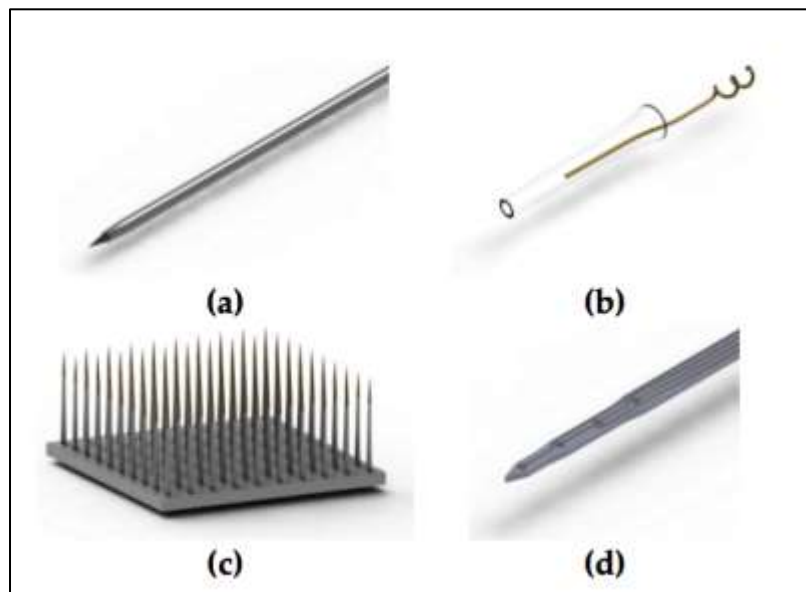Figure 2.5. Examples of different electrodes: (a) Screw electrode [28] (b) Wire electrode [29]

Figure 2.6. Hard electrophysiological interface (a) Microwire insulated with exposed tip (b) Glass cone with insulated wire (c) UTAH silicon based microelectrode array (d) Multisite Probe [30]

2.3.2.1 Microelectrode array:

Microfabrication offers various manufacturing advantages such as batch production, micro-scaling of electrode arrays, and helps to rapidly increase recording sites and resolution. Over the previous years, microelectrode fabricated by these techniques are being used for extracellular neural recordings and stimulation have been progressed from single electrode wires to microfabricated arrays. Even though microwires prove its robustness and functionality, one disadvantage is its mechanical stability. For example, the wires may bend during implantation. Related problems associated with wire electrodes make them unsuitable for long term stability and performance. The development of the fabrication processes for the integrated circuits consisting of photolithographic techniques with silicon etching technology makes it feasible for development and microfabrication of these microelectrode arrays. Photolithography enables the designer to create electrodes sites of micron size to match specific application. Microelectrodes can be advantageous for highly localized stimulation and recording of the neural tissue.

Figure 2.7. (Left) Kapton based 8-channel array [13], (Right) Micro-needle array [31]

2.3.2.2 High Density electrode array:

Spatial resolution in EEG recording is particularly important for precise measurement of synaptic delays or signal speed over relatively longer distances. Small inter-electrode distance is analogous to superior spatial resolution, which is a advantageous factor in most of multi-channel electrodes. This high spatio-temporal resolution tends to help to comprehend the brain activities in large-scale networks. Independent Component Analysis (ICA), a signal processing approach of finding independent components from a multivariable signal, is a common post processing technique in EEG data analysis. EEG recording is primarily composed of electrical potentials from different sources. Each source or a cluster of sources projects a unique topography onto the scalp and thus forms some type of 'scalp maps'. These scalp maps are added according to linear superposition principle. ICA attempts to reverse the superposition by segregating the brain signal into mutually independent scalp maps, or components with given or assumed scalp information and thereafter, from their geometry and conductivity properties within the brain, in most cases, current sources can be estimated [32].

In a 2010 study on 151 pediatric and adult epilepsy surgery patients found that Electrical Source Imaging (ESI) using 126–256 channels and individual brain MRIs as the head model yielded a sensitivity of 84% and a specificity of 88% in identifying the seizure onset zone. This was significantly better than that obtained using low-density EEG recordings [33]. In addition, increasing the electrode number adds to the physician time to visually review the data. Given these costs, determining the potential benefits

of increasing electrode number in pre-surgical evaluations becomes a matter of significant practical importance.
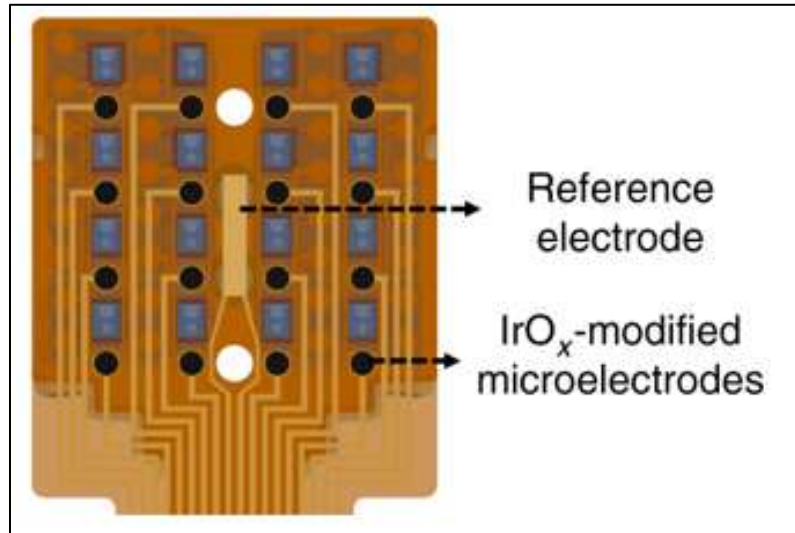

Figure 2.8. 16 channel Optoelectronic interface [34].

2.3.3 Hard vs. Flexible Electrode Design

Hard or inflexible electrodes can increase interfacial strains. *In vitro* studies further support the use for soft materials, indicating that softer substrates are more effective in promoting of cell growth than their stiff counterparts. When a piece of hardware is needed to be attached to the delicate tissue of brain or spinal cord, it is highly preferable for that piece of hardware to actually be soft, yielding, and flexible. The device is made flexible by replacing the silicon substrate with polyimide (PI). PI is polymer of imide monomer and comes in different types. It is flexible, biocompatible and a good insulator with high chemical and electrical resistances (resistivity in order of 10^{17} ohm and dielectric constants of 3.4). Due to these properties, PI has been generally used in

19

coating medical implants. PI can be spin coated and patterned with the same techniques as used for regular chip fabrication. This makes it ideal to create microelectrodes and combine it with metals.

Chapter 3: Device Design Considerations

Building process of the flexible 34-channel electrode consisted of three major phases – designing the electrode mask, selection of materials for different steps of fabrication and then fabricating this device using planned protocols.

3.1 Photo Mask Design for 34-channel EEG Electrode

The first step prior to fabrication is to design the desired pattern and transfer it to a mask so that this mask can be imaged during photolithography. A photo mask is a glass plate with transparent and non-translucent design on top of glass. Light can shine through the transparent part and blocked in the non-transparent parts of the mask.

3.1.1 AutoCAD:

AutoCAD is a commercial computer-aided design (CAD) software that engineers, architects and construction professionals reply on to design high precision 2D and 3D blueprints. It was developed and marketed by Autodesk Inc [35]. AutoCAD includes a variety of tools to draw object shapes such as circles, arcs, polygons, lines, 3D solids, and surface and mesh objects that allows for easy modeling of complex designs. The native file format for AutoCAD is .dwg and to make it more user-friendly, .dxf

(drawing exchange format) is also available to enable data exchange between AutoCAD and other programs.

3.1.2 Mask Design Steps and challenges:

The main target in our design is to allocate 34 channels in this very small area of 7mm x 11mm. The smaller the electrodes and lines, the more channels can be allocated in this small area. The main challenge was keeping the conducting lines thin enough so that it fits within this small area but also thick enough so that metal lines does not break during fabrication. Also, the polarity of planned photoresists need to be in consideration while designing the Mask in AutoCAD. In this design, all the circular electrode channels are equally spaced.

The design of the base of device has a shape similar to fingers which will cover the main regions of mouse brain. Finger shaped design is to ensure that we can put dental cement in the empty space to attach the final device onto mouse skull. Connection pads are maintained as thicker than conducting lines. The purpose of those connecting pads is to connect with external connector and its dimensions are chosen such that it can ensure an easy connection of the device to the external connector.

The fabrication will be a 3-step process, so the mask design followed similar steps. In first mask, we need to create the base and holes in it. Second mask design was done keeping in mind that the holes will be patterned with metal and additional metal line patterns will be used to make connections from electrode to contact pads. Third mask will be the top of the device which will be used to cover all designs as an insulating

layer except where we need to interface it with external circuit. Two additional masks were designed for patterning PCB in order to interface to external circuits. First PCB mask design is an interface between device which will be fabricated using first 3 designs and a commercial connector and the second PCB mask is another interface of 15mm length stripes from connector to create more separation between lines for easy handling during recording. These designs were then sent to mask company who made this 4" by 4" Iron Oxide Photomask which is used to transfer pattern during photolithography.
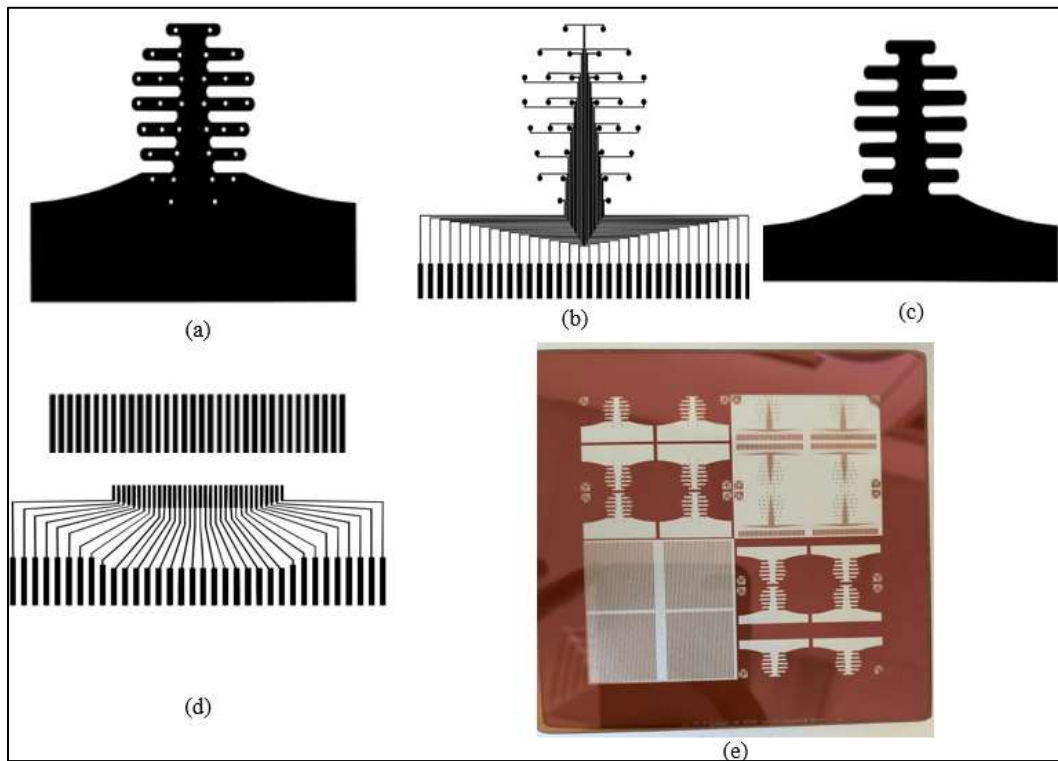

Figure 3.1. Photo mask AutoCAD design for 3-level fabrication. (a) It shows the first layer design with tiny holes in electrode locations. (b) Shows the Second layer with circular electrode pattern and connecting lines with them. (c) Last layer as a cover of isolation. (d) Designs for external connections. (e) Iron-oxide photo-mask.

Dimension selection: After few trials of fabrication, there was enough information to find the optimal set of dimension parameters. Dimension parameters were mainly

electrode diameters, thickness of the finger-shape structures and the thickness of the lines that are connecting the electrodes with external EEG equipment. A list of dimensions is shown in the table below.

Table 3.1 Design Dimension Parameters for AutoCAD Design of Electrode

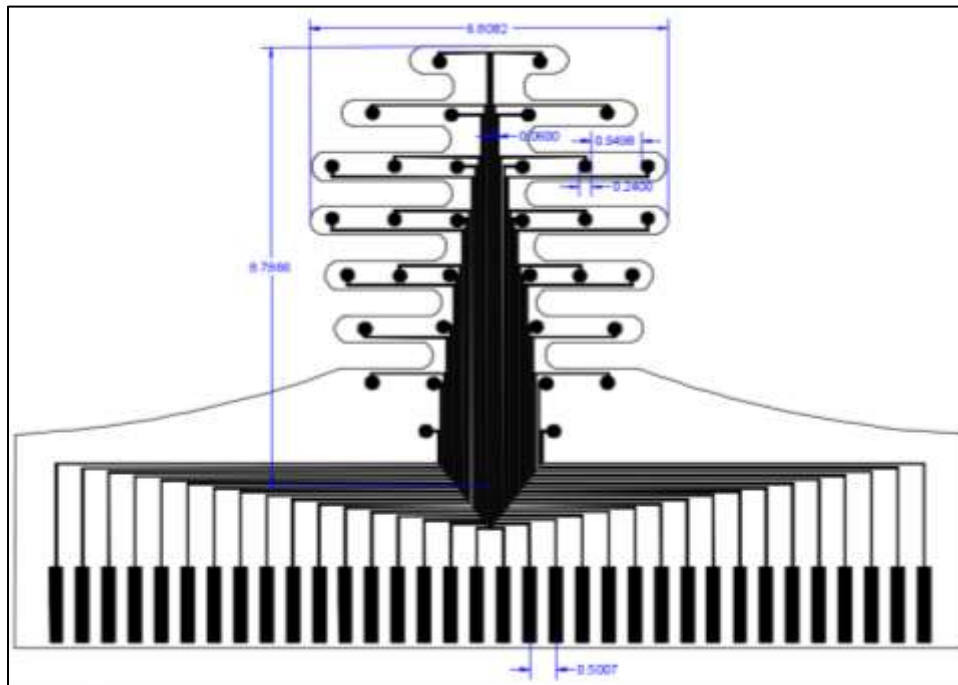| Parameters	Dimensions (in micrometers)
Device length	11000
Device width	7000
Finger width	600
Electrode diameter	140-240
Distance between two electrodes	950
Conducting lines width	35
Distance between lines	60
Area of contact pads	250*1500
Pitch of contact pads	500

Figure 3.2. Combination of 3 mask designs with dimensions

24

3.2 Materials

In EEG recording, electrodes primarily measures the potential between solid metal and electrolyte solution. To achieve better stability, properties of implant electrodes must be evaluated for biocompatible application and need to ensure optimum stability, efficacy, and lifetime with a very low to zero level of toxicity. Other requirements include, but not limited to, low separation at the boundary of electrode and electrolyte, low electrode impedance, biocompatible material coating accepted by the body, extensive performance and material stability for long time, no deterioration with excellent bio-stability. We have designed our EEG electrode device based on flexible substrate Polyimide, which is a photosensitive Polyimide named Duramide 7510 (Fujifilm). The other chemicals used were Duramide developer (QZ3501), photoresist AZ5214, AZ400k developer, gold, gold etchant, hydrofluoric acid, Kapton film, ferric chloride.

Durimide 7510 and developer QZ3501

For few years Polyimide (PI) has been used for neural implants such as neural prosthesis as a substrate/base. Photosensitive PI are advantageous because they offer simpler processing compared to non-photosensitive PI as they need photoresist which increase the processing time. They can act as a substrate to metal layers and in addition to that also serve the purpose of an insulator between metal and liquid of the body. PI is suitable for wide range of application on a wide range of substrates. It is an excellent material for biocompatibility and micro fabrication. In this project, the main reason of

using polyimide as the base is its flexibility, biocompatibility and its lightweight benefits. Photosensitive polyimides has the advantage of patterned for photolithography, solvent developable.

Few commercial photosensitive polyimides that are available are HD microsystem PD series, Toray Industries PW-1000 series, Fujifilm Duramide series. Among them we chose Fujifilm Duramide 7510. Its coating thickness ranges from 3 to 15 µm which is adequate for neural electrodes and its good biocompatibility has already been shown *in vitro* study [36]. In comparison to other conventional flexible materials, such as non-photosensitive polyimide and Parylene-C, photosensitive polyimide provides similar good dielectric properties but with excellent thermal stability and high flexibility, good mechanical and electrical properties [37].

Parylene-C

Parylene-C is another alternative to Polyimide. Parylene oxidizes at temperature greater than 100 degree Celsius. But during fabrication it have to go beyond that temperature like soft and hard bake, soldering sputtering metal and annealing thus make Parylene burn. Besides, Parylene based microdevices shows water diffusion through it. Also, poor adhesion to metals made it not a very good choice for bio implantation [38]. In addition to these, since this is a non-photosentive polyimide it needs to go through more complex fabrication process which is time consuming and brings more variability in fabrication yields.

SU-8

Although initially developed as a sacrificial, negative photoresist in the electronics industry, SU-8 has reemerged in biomedical research applications. SU-8 can easily be patterned to be thick, with high-aspect ratios, which make it amenable to use as a mold for other structures such as microfluidics or as a core material for neural probes [39]. SU-8 is "mildly reactive" according to ISO 10993 standards [40]. We should note that SU-8 is not a supported material for *in vivo* use by the manufacturer and it is not found in any known FDA approved implant [40].

Polydimethysiloxane (PDMS)

PDMS has been widely used in microfluidic and non-penetrating neural arrays applications. Photo-patternable PDMS formulations have not been fully evaluated for biocompatibility. Out of the many formulations of PDMS that exist, several are medical grade and commonly used in FDA approved medical devices and implants. Some examples include deep brain stimulators and ECoG arrays. Some studies have yielded evidences indicating that the curing agent may be toxic. As a result, users are advised to mix, cure, and sterilize their PDMS thoroughly before using it for a biological application.

Table 3.2. Physical properties of silicon and other flexible materials [30, 41-42]

Physical properties	Photosensitive material	Non photosensitive material				
	Duramide 7510	Si	Parylene-C	Polyimide (PI 2611)	SU-8	PDMS
Tensile Strength [MPa]	215	12013	68.9	350	-	-
Young's Modulus[GPa]	2.5	190	2-5	8.5	2.87-4.40	3.6×10^{-4}-8.7×10^{-4}
Glass transition [°c]	285	none	87-89	>400	200	250
Volume resistivity[Ωcm]	$>10^{^6}$	none	$>10^{^6}$	$>10^{^6}$	$> 1.5 \times10^{-16}$	
Dielectric constant	3.3 1MHz	12 1KHz	3.1 1Khz	2.9 1MHz	3.2	2.6-3.8
Water Absorption	0.06	none	1.08	>0.4	0.65	
Achievable film thickness	1-15	-	1-100	-	1-300	10-100
Biocompatibility	Yes (in-vivo)	-	USP Class VI	-	Mild reactivity (in vivo)	USP Class VI

Materials that meet USP Class VI standards, are expected to ensure a high quality level and better acceptance with the FDA and USDA because the materials are believed to substantially reduce the risk of causing harm to patients from reaction to a toxic material.

Gold

Gold (Au), Ir, Pt are widely used materials in producing neural electrodes for the individual recording microelectrode sites, interconnect lines and connection pads. Titanium can oxidize in the body, For this study, we have chosen Gold (Au) as the

electrode conducting material because of its low resistance, flexibility and biocompatibility [43]. Gold has a high conductivity (4.10* 10^7 S/m), is corrosion resistant and biocompatible for use of neural environment. With a Young's Modulus of 78 GPa, Au has enough flexibility for neural electrodes compared to Ir, Pt whose respective Young's moduli are 529, 1532 GP. With this flexibility, the electrode will be able to follow brain movement to a greater extent without fracturing. Due to low adhesiveness between Au and polyimide, the surface of polyimide was made rough to improve Au adhesiveness [41]. In case of platinum it showed difficulty in deposition in polymer film [44].

AZ5214 Photoresist and AZ400 K developer

It is a positive pattern photoresist used in our fabrication to pattern gold. The benefit of using this photoresist is that its thickness can be modulate by controlling the spinning speed. It can also be used as negative photoresist.
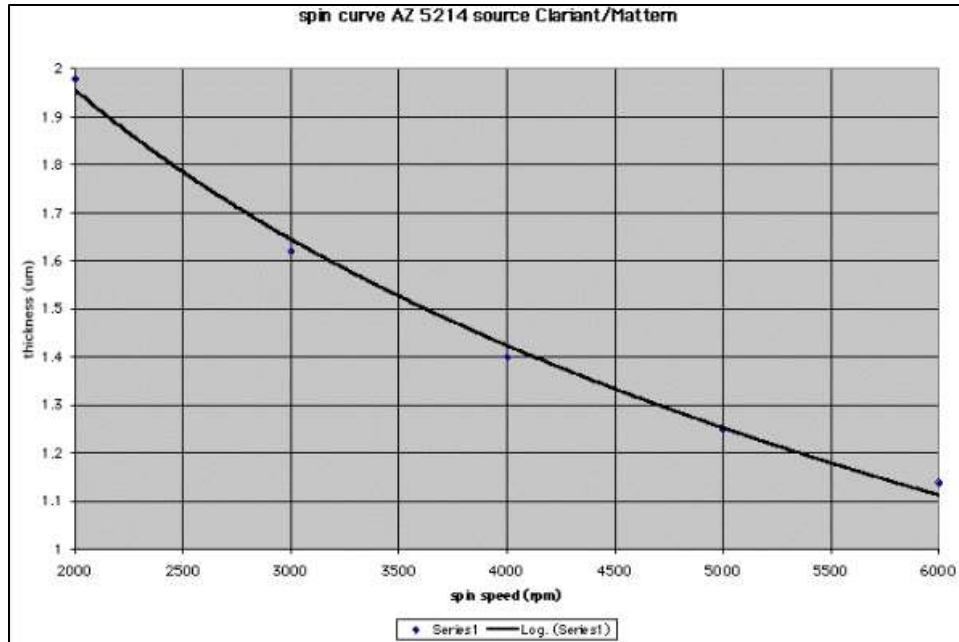
Figure 3.3 Spin curve of AZ5214 [45]

Hydrofluoric acid

Hydrofluoric acid is the only etchant which attacks amorphous SiO_2, quartz, or glasses at significant high etch rate. It is used to etch sacrificial layer silicon dioxide in our experiment. [44].

$$SiO_2 + 6HF \Rightarrow H_2SiF_6 + H_2O$$
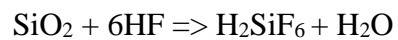
Since HF is severely hazardous if it comes in contact with skin specific chemical safety guidance have to be followed.

3.3 Finalizing the Design

Keeping in mind which chemicals will be used mask was designed. For example in our design we are going to use Duramide which is a positive tone resist and AZ5214 is a negative tone resist, which means for AZ5214 exposed area will be developed and for Duramide exposed area will not be developed and stay, so the design will follow the polarity of each chemical. Another important factor was to ensure that mapping of layer 1 to 3 are accurate before sending the design to make the mask. After rechecking the finalized design from AutoCAD it was then sent to the mask company as a .dwg fie. Later these masks will be the master copy of what we need to pattern during fabricating our microelectrode array mouse EEG device.

Chapter 4: Device Fabrication

In this chapter, the various steps of fabrication process and achieved outcomes at those steps are described.

4.1 Fabrication of EEG Electrode Array

EEG electrode fabrication processes will be described in next few sections.

4.1.1 Clean Room Protocol

Standard photolithographic clean room procedure was followed during microfabrication. The thickness of the final 34 electrode array is only 12 micrometers which ensures the reduction of bending stiffness. The length and width are 11mm and 8mm, respectively. In this section, fabrication process and results at each steps are described.

4.1.2 Major Instruments Used

The main instruments used in this whole fabrication process were Spinner, PECVD, JBA Contact aligner, RIE, Sputter, Mask aligner, profilometer, Annealer.

    a. Spinner provides a means to apply photoresist or any other polymer by using vacuum and a programmable set of parameters that control speed and spin duration. It can deliver different thickness of photoresist by varying the speed

and duration of the spin. Related speed and timing of spinning is provided in fabrication steps section.

b. Plasma enhanced Chemical Vapor Deposition (PECVD) is a widely accepted technique within industry particularly for depositing thin films from a gas state to solid state on a substrate. In PECVD plasma energy, as well as thermal energy drives the reaction between excited electrons and substrate.

c. Sputtering is a process where microparticles are ejected from a source material that is to be deposited on a substrate.

d. JBA Contact Aligner is a light source and flood exposure system. This is used for fine line patterning on substrate as per the design provided.

e. Reactive-Ion Etching (RIE) is a type of dry etching by chemically reactive plasma to remove undesired materials form the surface of wafer. Plasma from gas that is pumped into the chamber generates high energy ions which collide the surface and the reaction etch the surface anisotropically.

f. Bruker Profilometer is used to measure surface profile such as thickness, roughness. In our fabrication it's being used during different stages to check the accuracy of previous step.

g. Thermal Annealer is useful for annealing in nitrogen environment where a process of heating and cooling to change the microstructure of material such as tensile strength, flexibility. Nitrogen is used because it is an inert and non-reactive gas.

4.1.3 Fabrication step-by-step Process

The step by step procedure of microfabrication of mouse electrode array is discussed below. The step flow, parameters like time, speed, amount of deposition was obtained after multiple trials and studying about material properties.
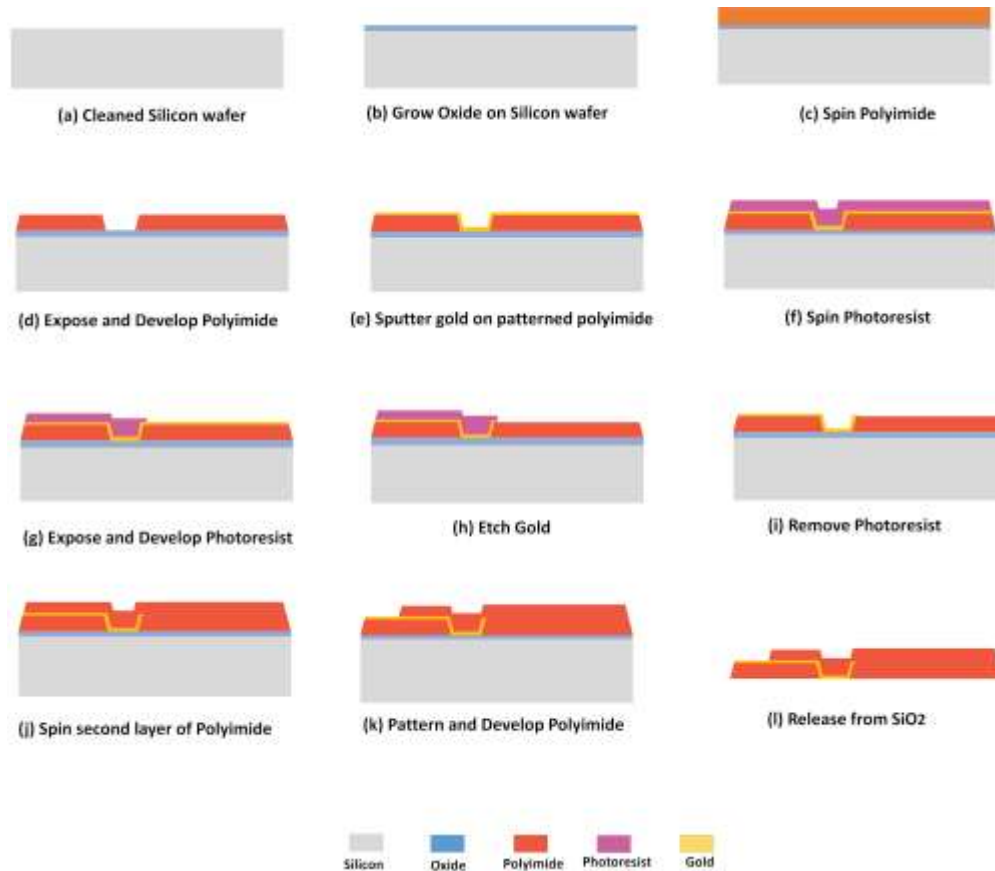
Figure 4.1. Layer by layer fabrication on silicon substrate

1. Fabrication started with a silicon (Si) substrate. At first to start with a clean surface cleaned it with acetone for 30 seconds and methanol for another 30 seconds.

2. The next step is to form SiO_2 layer on top of silicon substrate which will be used as a sacrificial layer to release the final device from Si substrate. PECVD is used to grow 350nm thick layer of oxide.

3. Hot bake at 140 degree Celsius for 3 minutes. Now Spinner is used to spin first HMDS and then Duramide at 3000 rpm (revolution per minute) for 40 seconds.

4. Prebake at 100 degree Celsius for 4 minutes. JBA contact aligner is used to align the substrate to the first mask design with openings at the place of electrodes. A 40 second of exposure creates the pattern on the substrate.

5. Post bake for 4 min at 100 degree Celsius. Then develop with QZ3501 developer to open the electrode sites. It will take around 30-40 seconds to see the desired design on top of polyimide. The microscopic view of the outcome after this stage. When the desired pattern is visible dry it with nitrogen spray gun.
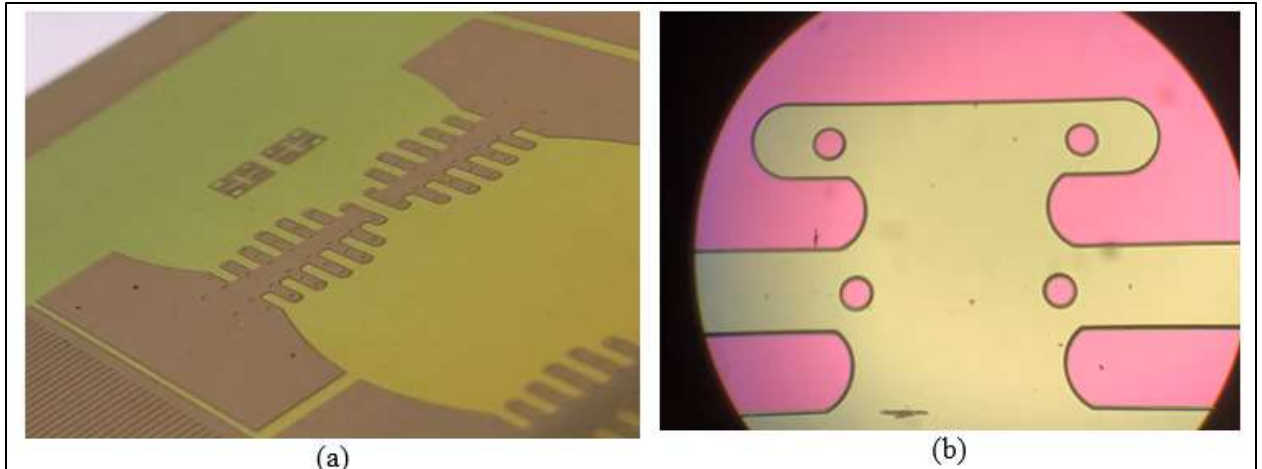
Figure 4.2. (a) Polyimide base on silicon wafer, (b) Microscopic view of base layer of polyimide.

6. Curing is performed in nitrogen environment for 30 minutes. The annealing temperature of duramide is 350-degree Celsius.

7. Gold deposition is the next step. But the problem with gold is that it does not have good adhesion with polyimide. To increase the adhesion of gold with polyimide the method I followed is to roughen the surface of polyimide which makes gold to adhere more strongly. Before that gold will peel off from polyimide where it was exposed. Roughening the surface is done by RIE using oxy plasma at 250watt for 10min. It will give a bump surface on top of polyimide which had a height of 10-20nm. Profilometer is used to check the roughness as shown in figure below.

36
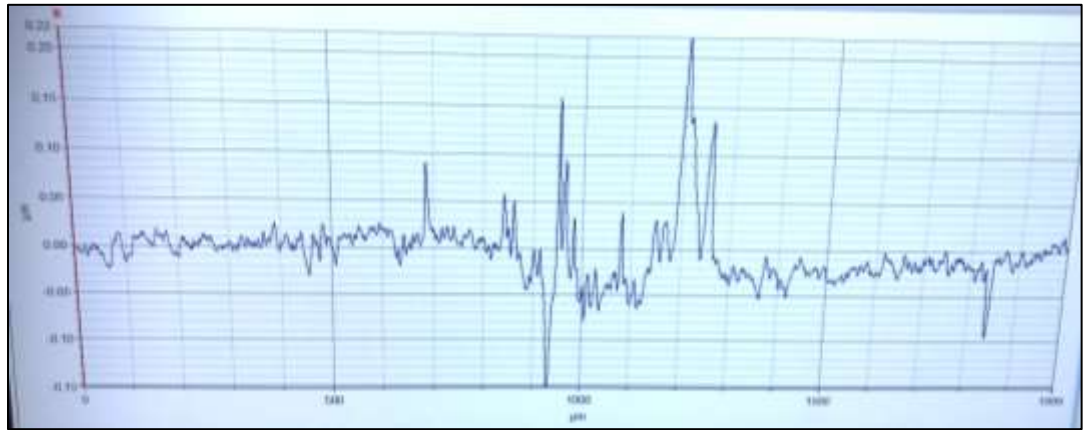
Figure 4.3 Measurement of surface roughening before gold deposition.

8. In next step, a 5000 Angstrom gold layer was sputtered in 25 minutes. 2 min hot bake will complete the gold deposition step.
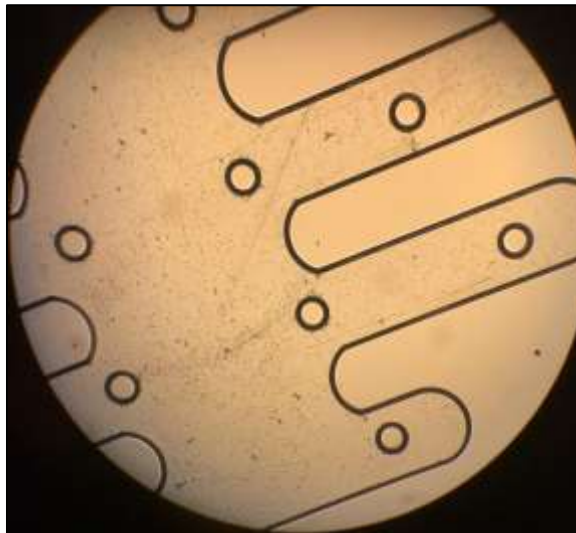
Figure 4.4. Microscopic view of Gold deposition

9. AZ5201 photoresist was spun at 2000 revolution per minute. Here the spinning speed is kept low to have a thicker photoresist layer.

10. Mask aligner is used here to align the 2nd design on photomask with filled up electrode holes and contact lines. A careful perfect alignment will ensure that the contact lines fall inside the 1st polyimide layer and also we can form metal electrodes through the holes of 1st design.

11. The photoresist is then patterned by UV lithography for 20 seconds and developed about 35 seconds with AZ400k developer to generate the metal layer pattern on photoresist. Make sure to mix AZ400k developer with DI water in 4:1 ratio. When the desired pattern is visible on photoresist wash it with DI water and dry it with nitrogen spray gun.

12. Undesired gold was then etched away using gold etcher for 3 minutes, after checking the lines individually from electrode end to contact pad end under microscope so that there is no breakage of gold lines the next step of photoresist removal is performed. Photoresist was removed by keeping the sample in acetone for 1 minute and then wash and dry as usual. Thus, a desired metal pattern was left on top of bottom polyimide.
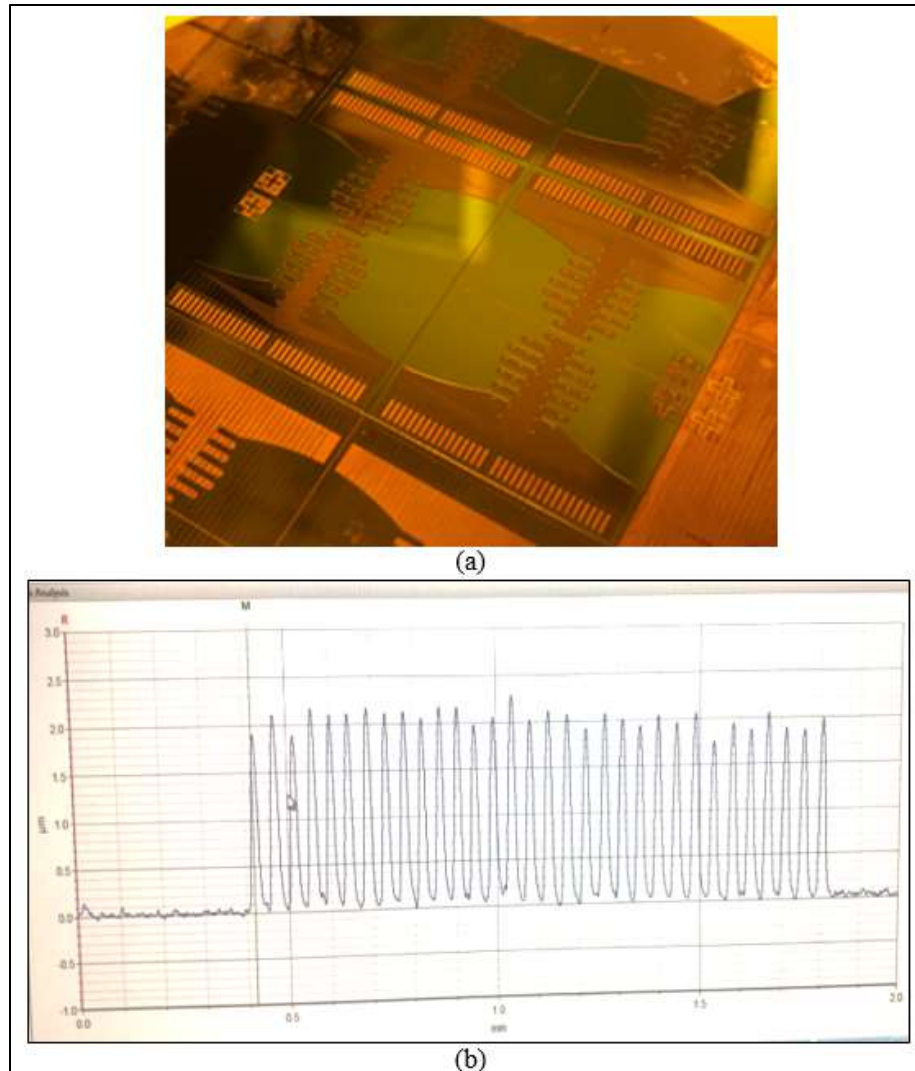
Figure 4.5. (a) Metal Pattern on top of Polyimide (b) Metal thickness measurement of each lines

13. Next, a top polyimide layer was formed using the same method of bottom polyimide layer but aligning the 3rd design this time. This layer was to insulate the electrodes and contact lines from top leaving the bottom contact pads exposed for external connections.
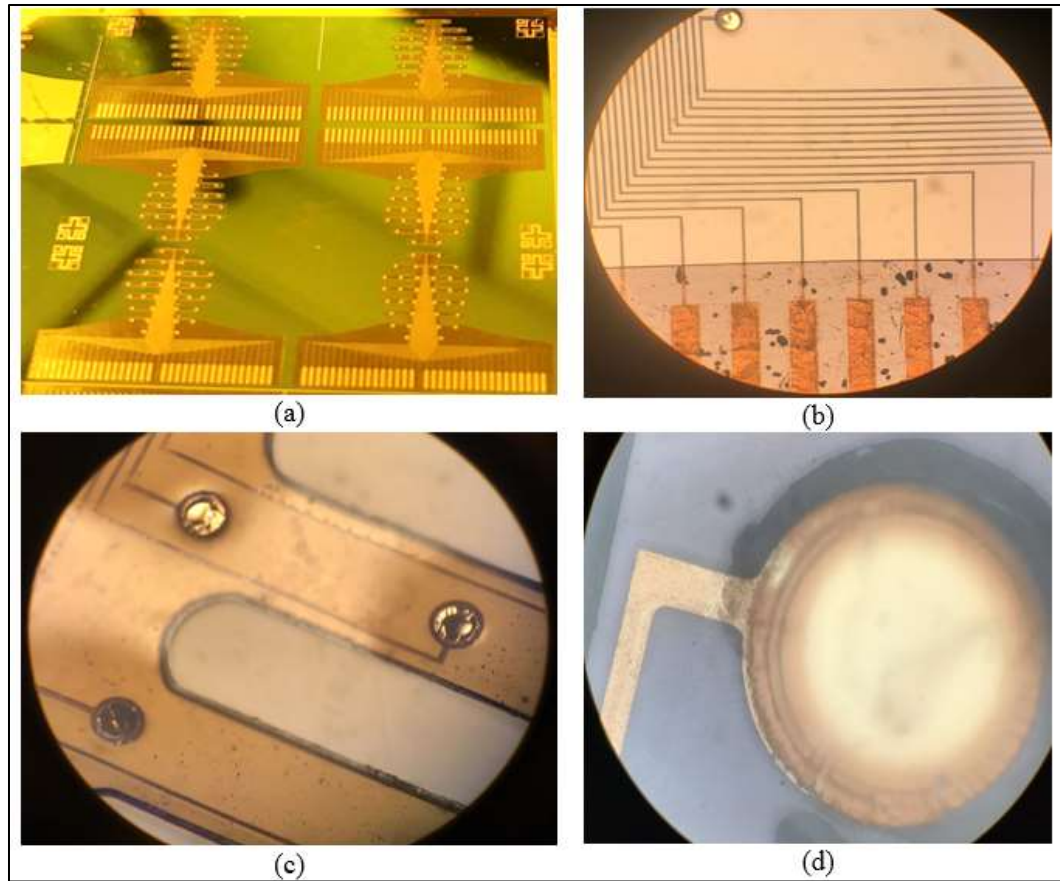
Figure 4.6. (a) Final layer of patterned Polyimide (b) Microscopic view showing the exposed contact pads, (c) Microscopic view of the electrodes under the Duramide cover (d) Microscopic view of a single electrode.

14. The sample is then again dry etched using RIE to remove any remaining polyimide from the undesired area, at this point which is the lower part of the device. If any polyimide is still there it would be hard to connect this with external circuits.

15. Cure it in nitrogen environment at 350-degree Celsius for 30 minutes.

16. Dip the wafer in Hydrofluoric acid (HF) to peel off final 34 channel electrode array from the silicon dioxide wafer. The final device is shown in Figure 4.7.

40
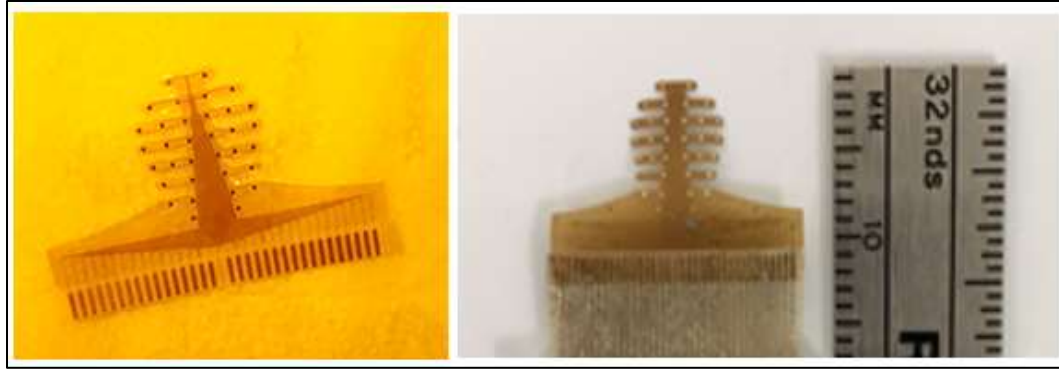
Figure 4.7. Final 34-channel mouse EEG microelectrode array
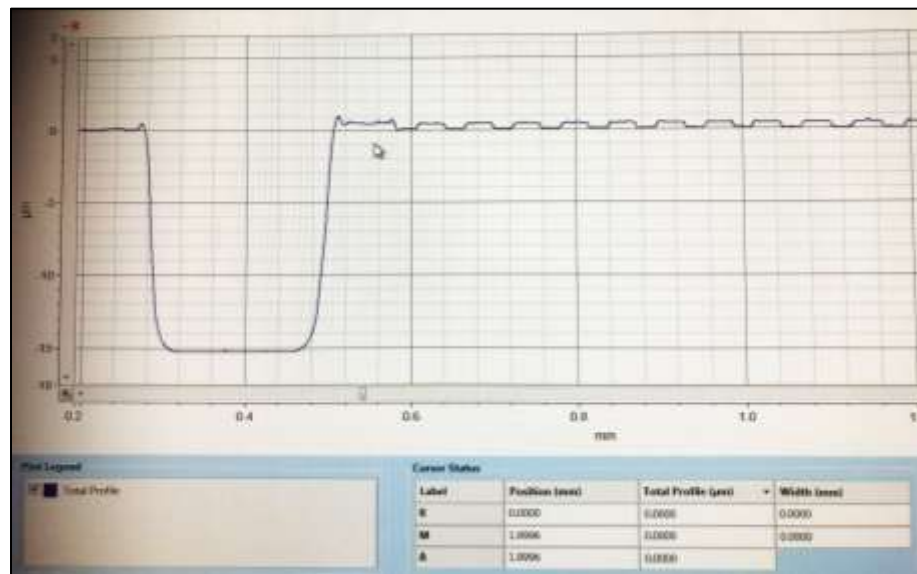
Figure 4.8. Measured thickness of the final device

Benefit of curing

The main objective of proper PI curing process is to complete the imidization process of PI. If the imidization process is not controlled properly there can be localized mechanical stress variation across the PI. This curing process was done in nitrogen environment at 350 degree Celsius for 30 minutes because oxygen from air can darken the PI film. Film transparency is critical when multiple PI layers are used during

41

fabrication for proper alignment. Curing process also removes the residual solvents and

photosensitive components and optimize film adhesion performance.
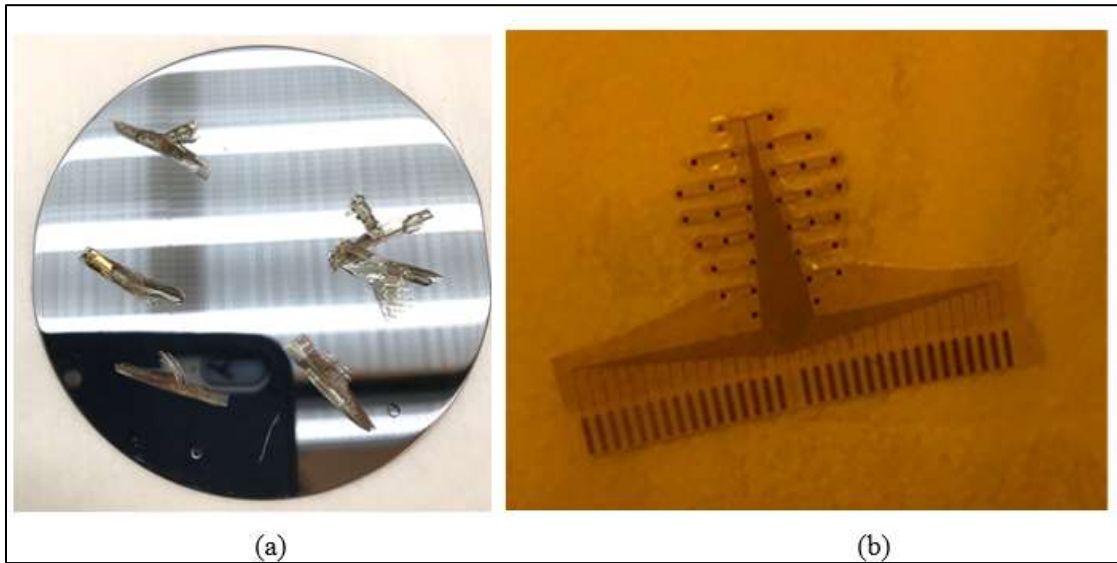
Figure 4.9. (a) Without curing (b) After curing

Benefit of surface roughening

In this experiment I have seen dramatic increase in the adhesion strength after surface

morphological roughening through plasma reactive etching between Polyimide and Au.

Figure 4.10 shows the weak adhesion between PI and metal (Au) before increasing the

roughness of PI surface.

Figure 4.10. Without doing surface roughening before gold deposition, detachment of metal from Polyimide is clearly visible

4.2 Printed Circuit Board Fabrication on Kapton film

For the purpose of connecting the polyimide microelectrode array to external circuit it is necessary to connect it with something hard but not heavy printed circuit board (PCB). We used Kapton film for this purpose because of its light-weight and flexible property. Two sets of design are then fabricated on top of it. The 1st PCB is of straight lines which is designed in the purpose of connecting contact pads of electrodes with chosen connector thus providing a platform on which the array components can be mounted, keeping in mind that the spacing of PCB lines matched with both contact pads spacing and connectors spacing. The 2nd PCB is for widening the 34 connections lines so that it would be easier to solder long wires easily which will be later connected with input ports of data acquisition system.

4.2.1 PCB Fabrication step-by-step Process

The Fabrication steps of these two PCBs are described below.

1. Cleaned Kapton films with acetone and methanol for 1 minute.

2. After prebaking the films at 90°C for 2 minutes, spin photoresist AZ5214 at
   4000 rpm for 40 seconds. And then post bake the kapton film at 120°C for
   another 3 minutes.

3. Aligned the mask designs on this film and expose with UV light for 25 seconds.

4. Developed with AZ400K for about 40 seconds until the desired pattern is
   visible.

5. For this step, Ferric Chloride ($FeCl_3$) is used to etch away undesired copper
   from it and thus pattern the film in desired design.

6. Finally, acetone is used to remove the remaining photoresist.
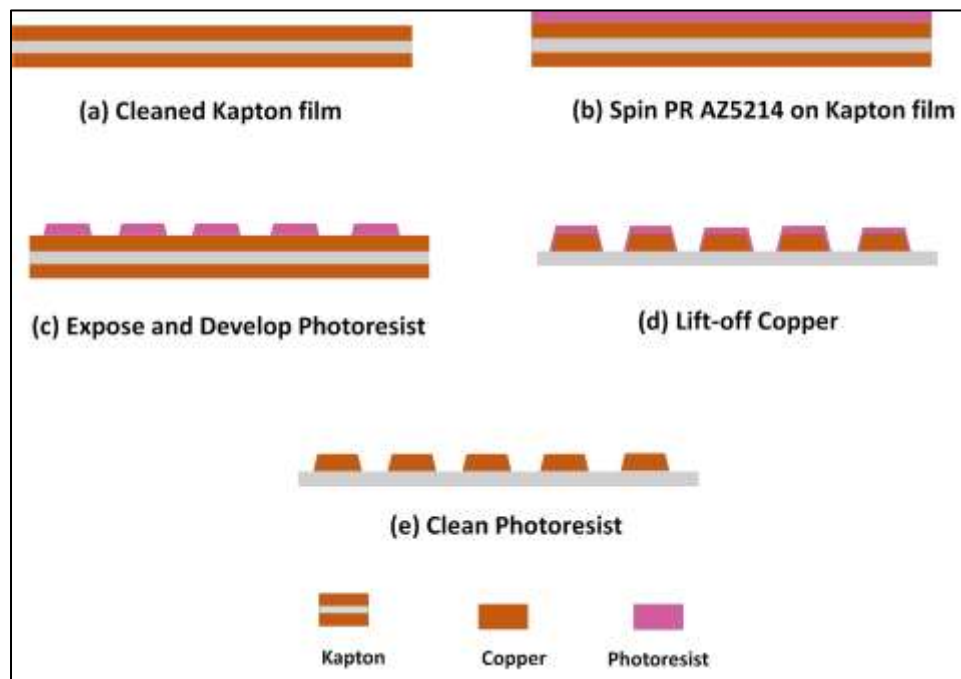
Figure 4.11. Layer by layer PCB fabrication on Kapton substrate
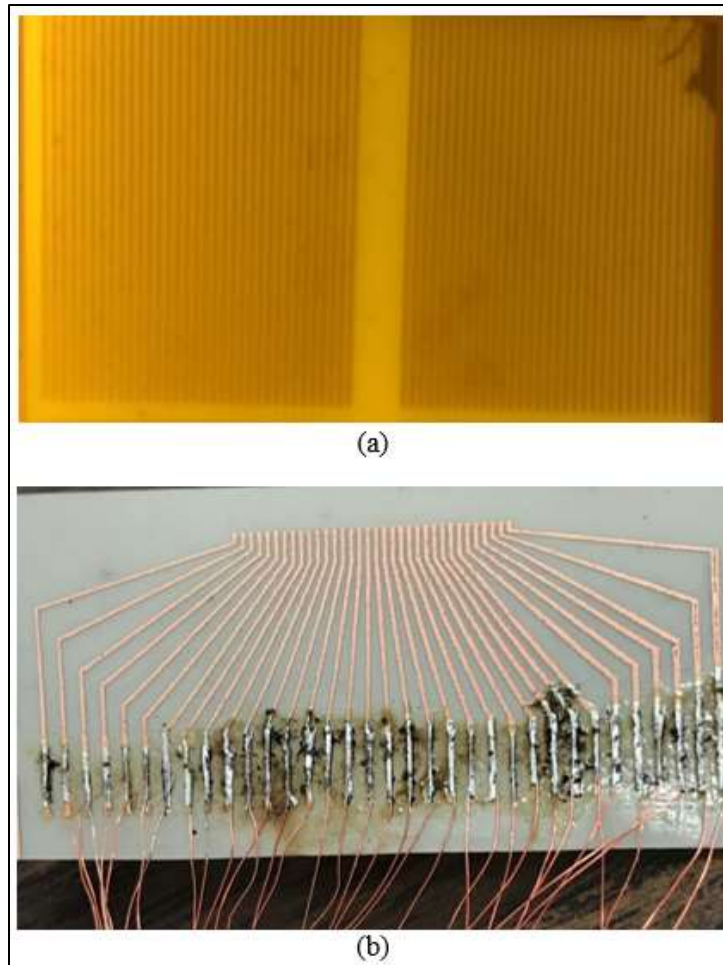
Figure 4.12 Fabrication of 2 PCBs

4.3 Challenges during Fabrication

4.3.1 Shrinkage effect:

Polyimide tends to shrink during curing process after all the fabrication was done but through incorporating additional time sensitive curing steps it was found that if polyimide is being cured not after the peel off from oxide but after each time polyimide is being formed the shrinkage can be avoided. In previous section, Figure 4.9 shows the effect of curing. Since the external PCB is designed based on the pitch in

45

microelectrode array on polyimide it is checked and confirmed that this procedure can avoid shrinkage of polyimide.

4.3.2 Gold Adhesion:

For various reasons discussed earlier we used gold as our conducting material. But the problem with gold was that it does not adhere with polyimide very well which result in broken connecting lines and connecting pads. The method we followed here to avoid this problem is by making the polyimide substrate surface rough enough so that the adhesiveness with gold increase.

Chapter 5: Device Testing and Interfacing

In this work, major focus was to finish the design and implementation of the 34-channel electrode and a significant portion of time was spent in optimizing the design and fabrication process to build the final electrode. Therefore, a limited amount of testing has been done the device and some of the remaining testing are outlined as next step or future work. The next sections of this chapter briefly describes the work completed in testing the conductivity of the electrode array and its interfacing to removable connector.

5.1 System Block Diagram and Device Testing

The block diagram of full system is shown below. Here it shows how the developed electrode will be used in the bigger picture. As an immediate next step, electrode needs to be interfaced with removable external connector so that it can be connected to the data acquisition system for amplification, filtering and acquisition to the computer system.
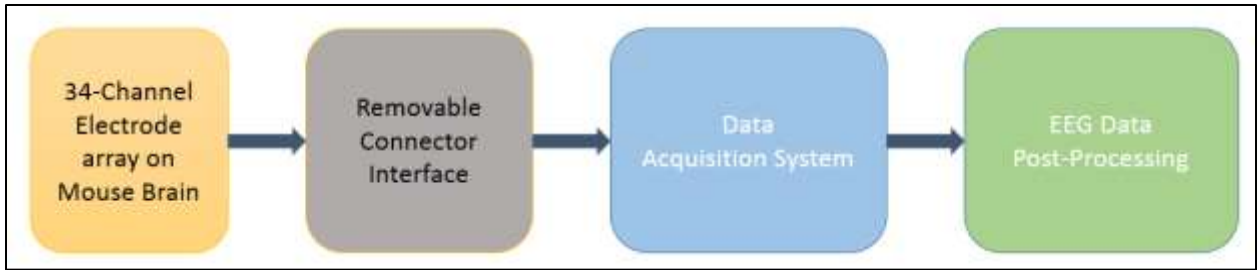
Figure 5.1 Block diagram of full EEG acquisition system

The objective of designing the PCB is to adapt the spacing of microelectrode array connection pads to the spacing of the chosen connector and providing a platform on which the array components can be mounted.

After the electrode was fabricated, an important step was to validate the quality of connection for all electrodes. A test has been done to determine the connectivity of each electrode. This is done by putting the flexible electrode device on a gold metal plate so that all the electrodes will touch the metal plate, the same way it would be done on mouse. A connectivity test in then performed using a Digital Multi-Meter (DMM) from the output end (that is the connector pins) which shows that output end is receiving signals from input.

Out of several batches of built devices, resistance was mainly measured in final two sets of devices. Measured resistance for electrodes were ranging between approximately 120-480 Ohms in first set of 6 devices and approximately 60-80 Ohms in second set of 6 devices. This was measured between a metal surface that was in contact with all the electrodes and the connector pins on the other side of electrode.

The variation in measured resistances is most likely from measurement error due to lack of flexibility in probing very small pins of connector.
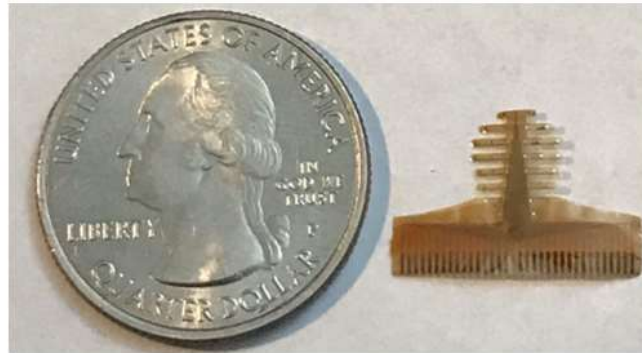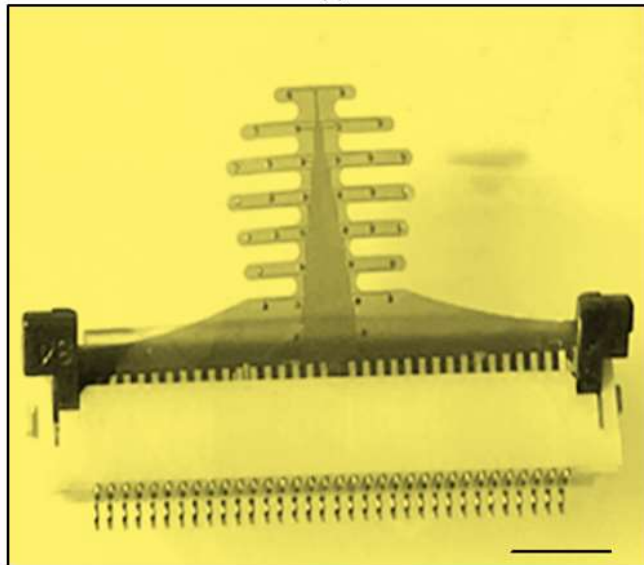
Figure 5.2. (a) Final Device, size in comparison to a US Quarter Dollar coin. (b) Direct interfacing of 34-channel electrode to a connector. Scale bar: 2.5mm.

However, for mouse recording application, the above interfacing setup may not be practical. Keeping the relatively heavy weight connector so close to electrode and carrying the load on top of the mouse brain may cause tension to the electrode and there is a risk of getting the device disconnected from the connector. Therefore, we have devised a better approach which is shown in Figure 5.3. A Kapton film, which went

through the process described earlier in Section 2.4 and it has 34 straight lines that is designed to conduct the signal from one end of film to the other end, is inserted between the electrode and connector. The top end of the film is to receive the endpoints of electrode, either soldered or tightly taped, and then the other end is inserted into the connector, as shown in Figure 6. This will ensure the connector is safely at a distance from mouse brain recording site.

5.2 Device Interfacing to External Connector

5.2.1 Step-by-step Process

The interfacing of two PCBs with commercial 34 pin connector and 34 channel PI microelectrode array is described below.

1. 34-channel electrode array was interfaced with first PCB.

2. The ends of first PCB will go inside the 34 pins connector with 0.5mm pitch.

3. Connector male pins were then soldered with the second PCB as shown in Figure 5.3(a).

4. 34 long wires are soldered with the other end of the second PCB as shown in Figure 5.3 (b)
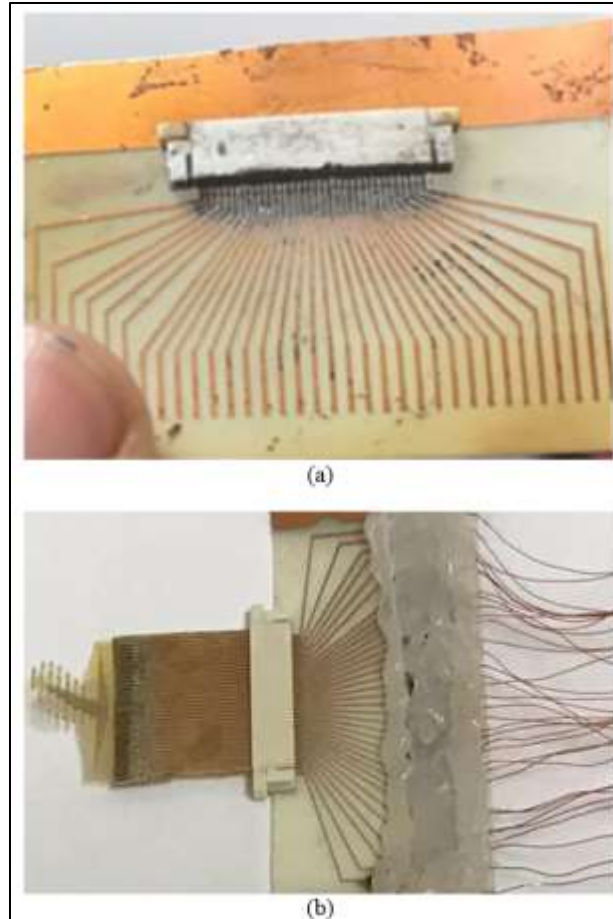
Figure 5.3. Interfacing of 34-channel electrode via a Kapton film to connector and subsequent soldered wires. (a) Soldered connector with PCB, (b) All the interfaces

Figure 5.4. Setup for measuring resistance of each electrode after the device was soldered onto the interfacing PCB at the connector pad end

Finally, these wires will be connected to an Analog to Digital Converter (ADC) where we will get the desired EEG signal. The external connections were done in such a way so that the external wiring can be removed from the connector, when the device is not being used for recording EEG.

5.3 Device Testing for Signal Transmission

One important test was to check the quality of signal propagation through the electrode. If we provide a known signal at the 34-channel electrode, by recording the signal at the connection pad or at the rear end of the interfaced PCB will validate the quality of signal transmission through the electrode. This is basically treating the device as a low resistance connecting wire and it will test two things: (1) if the electrode is broken, no signal will pass through to the scope. (2) if the electrode impedance is very high (~MOhm), once connected to a 1MOhm scope, the detected signal be almost half of input amplitude. But if the impedance of the built device is very low, there is minimum voltage drop at the device and the detected signal at the scope will have almost equal to the voltage amplitude as input.

5.3.1 Setup of Experiment

The setup of the measurement was very simple. At the electrode end, a signal generator was used as input source and on the interface PCB end, an oscilloscope was used to monitor the transmitted signal.
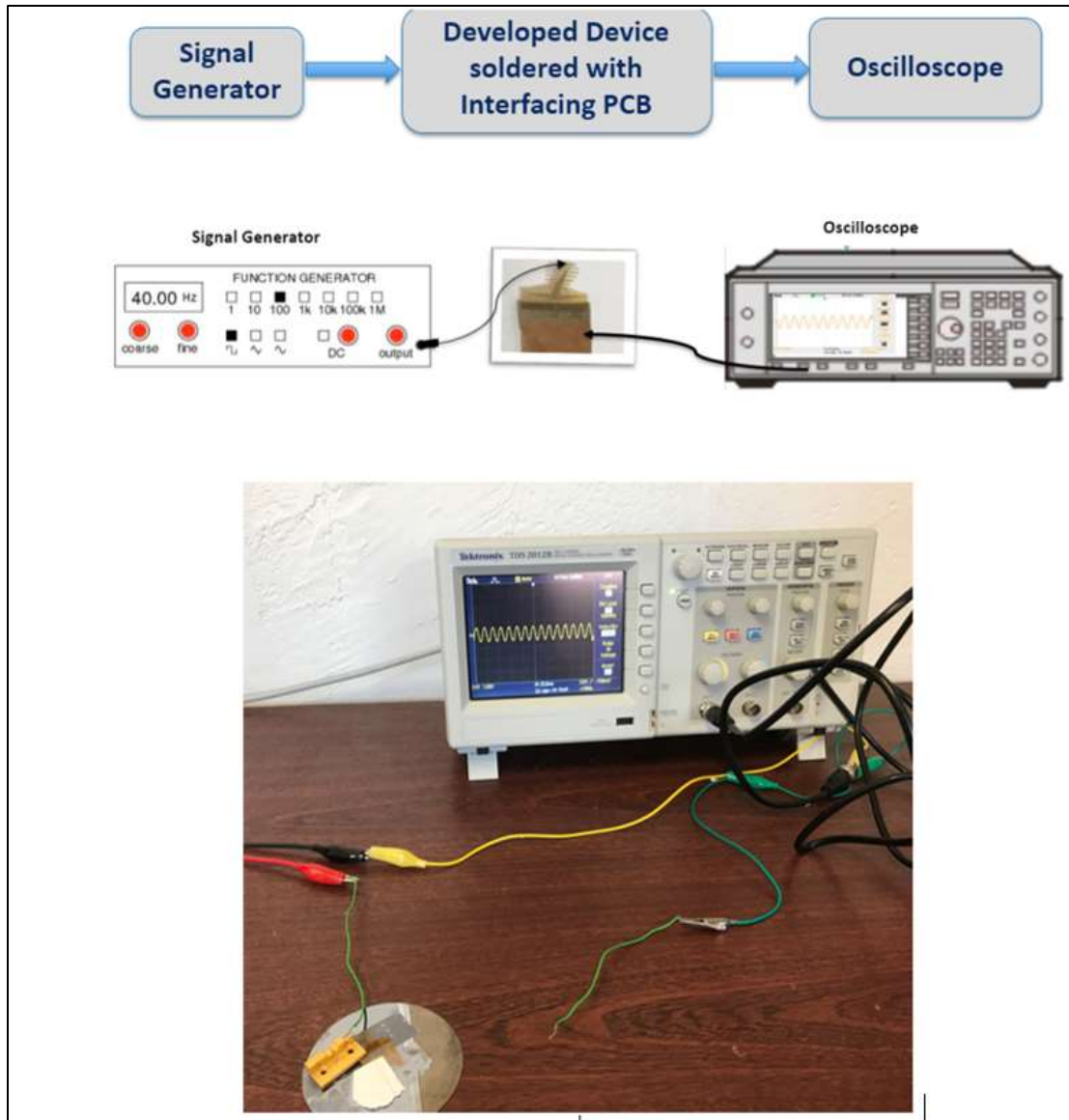
Figure 5.5. Setup for signal transmission measurement

5.3.2 Experimental Results

Once the signal generator was turned ON, there was signal visible on Oscilloscope showing the same frequency and almost same amplitude sinusoidal signal as the input. Here is shown a representative scope screenshot of transmitted signal when input from a signal generator was a sinusoidal signal of 1V peak amplitude and 40Hz frequency.
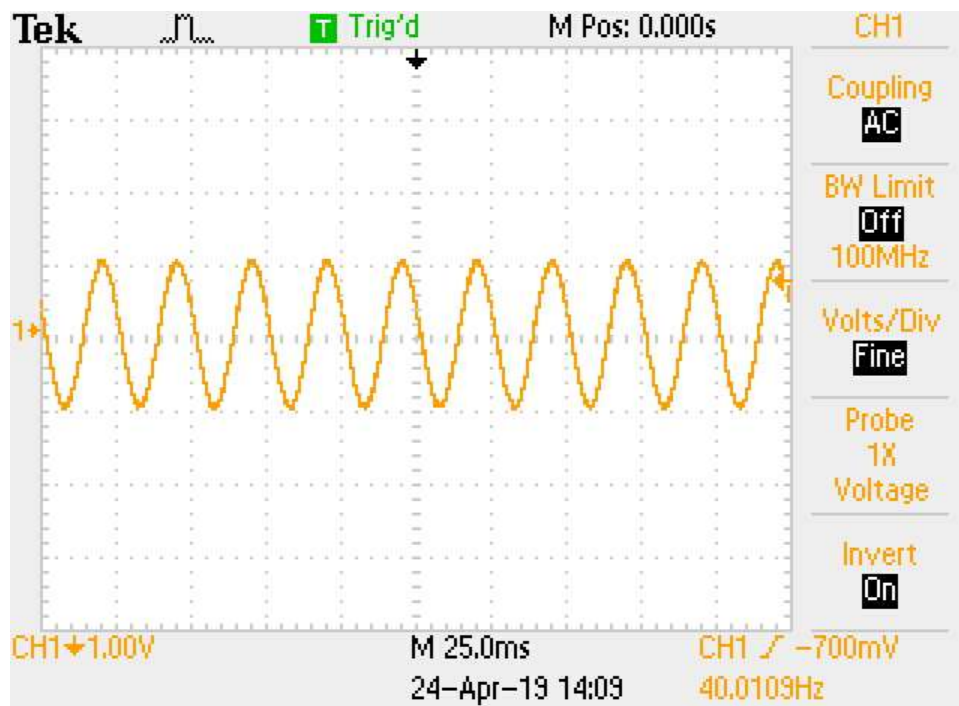
Figure 5.6. Transmitted output signal through the electrode as shown on an Oscilloscope. Input was a sinusoidal signal of 1V peak and 40Hz frequency.

Chapter 6: Conclusion and Future Work

6.1 Conclusion

In this work, a polyimide-based flexible 34-channel electrode was designed using CAD and then implemented its fabrication following step-by-step process. The specific goal of this thesis was to design and build this device and validate it so that it can be provided to the group for mouse EEG recording. Design work involved designing three layers of masks for the electrode device and then designing interfacing PCB that contains the connecting lines. After few iteration of design changes, final mask was ordered and fabrication was done at UMBC clean room following standard photolithography protocols. A key element of fabrication was choosing optimal materials prior to fabrication. Due to several advantages, both mechanical and biological, Polyimide (Duramide 7510) was chosen as the material for substrate or base material. Gold was chosen as the material for electrode due to its superior conductivity, biocompatibility and inert behavior.

After fabrication, electrode was interfaced with 34-channel connector by soldering the electrode end points onto the interfacing PCB. Once interfacing was complete, the device was tested to validate the channel quality for signal propagation. First test was to visually inspect the device for any damage or sign of losing gold from electrode points. Second test was done to measure the resistance of the device using a setup with

Multimeter. Third test was focused on validating signal propagation through the device by using a signal generator and an oscilloscope at two opposite ends of the device. These tests confirmed that the developed device has intact build, small resistance (~60-80 Ohm) and reliable signal propagation from its electrode points to the contacts pads.

As parallel effort for future work, data acquisition card was also setup to acquire the signals from this electrode and to execute subsequent analysis and post-processing. Next step of this work is to carefully install this electrode assembly on top of mouse model *in vivo* and then record EEG signals. We believe that increased spatial resolution of electrode channels in this new device will allow to obtain EEG signals with significantly reduced noise (through ICA processing) and therefore, enable us to record more meaningful and robust information from brain layers. In long term, this is expected to assist us in improving our understanding of brain activity.

6.2 Future Work

Future works can be allocated in few categories. As a continuation of this developed electrode device, immediate next step will be to complete the testing of all available devices and make a pool of them for use in mouse EEG recording. To enable mouse EEG recording, carefully installing the selected device on top of mouse skull will be an important step. Being a flexible polyimide-based electrode, while this will allow to attach it on the mouse brain and take its shape, there needs some pre-caution not to
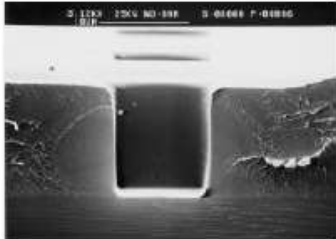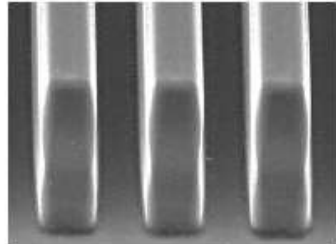
break the device. Once installed, the device will be firmly attached by using dental cement and that will make it very robust for subsequent recording sessions.

A second effort as future work can be some research on Chromium as a potential second material to be used with Gold. During some limited research of this work, there were interesting studies found that showed that using Chromium as a first layer of metal and depositing gold on top of it increases the strength of the bonding, therefore, provides increased adhesiveness. This will potentially help to ensure that the metals are attached well with polyimide. This, in turn, will help to make better connections with external circuitry.

A third line of effort is designing high density microelectrode array for use in rat EEG recording. Rat brain has more complex activity and has a better performance in cognitive and behavioral tasks than mouse, therefore, a better animal model for advanced neuroscience behavioral studies. Once designed and fabricated, that EEG electrode can be similarly used for recording activity from rat brains.

Appendix

Technical product information of Duramide 7510 (Polyimide):

TECHNICAL PRODUCT INFORMATION

FUJIFILM

Durimide® 7500
Photosensitive Polyimide
Precursor

- Designed with a unique structure and sensitizer that gives it the following characteristics:

  Fast photospeed
  Enhanced resolution
  Wide process latitude
  Self priming
  Excellent adhesion

- Superior mechanical property retention after extended pressure cooker test (> 1000 hour)

- Cured film thickness range: 2-50µm

Type	Viscosity	Cured Film Thickness
Durimide® 7505	1200CS	2-5µm
Durimide® 7510	3300CS	4-15µm
Durimide® 7520	6400CS	11-25+µm

Compatible Ancillary Products:

Developer/Rinse Combinations : Back Side Rinse:
QZ3501/QZ3512   QZ3501
HTRD2/RER600   HTRD2

Edge Bead Remover :   Stripper Products:
HTRD2   N-Methyl 2-Pyrrolidone
                       QZ 3322

Cured Film Properties of Durimide® 7500 Series

Property	Unit	Value
Tensile Strength	MPa	215
Young's Modulus	GPa	2.5
Tensile Elongation	%	85
Glass Transition Temperature	°C	285
Thermal Decomposition Temperature	°C	525
Coefficient of Thermal Expansion	ppm/°C	55
Dielectric Constant		3.2-3.3
Moisture Absorption@50% RH	%	1.08

Contact print resolution mask in 40µm softbake film

10µm via in a 10µm softbaked film, i-line stepper

12µm lines and spaces in a 44µm softbaked film, g-line stepper

FUJIFILM ELECTRONIC MATERIALS

Process Window

Exp.Range   60-200mJ/cm2

Focus Range	4-8 microns into film
Substrate:	Silicon
Soft Bake:	100°C /3mins
PI Thickness:	12µm
Exposure Tool:	Canon i-line stepper 0.6NA , 0.5 sigma
Post Exposure delay:	20-22°C/ 30 mins
Developer/Rinse:	HTRD2/RER600 30"/10"/15"
Cure:	350°C/ 60 mins
Cured Film Thickness: 6.2 µm	

Characteristic Curve
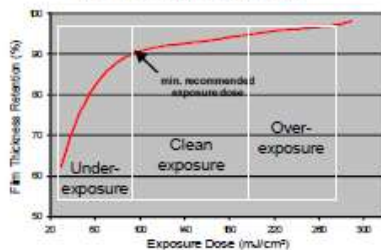
Process Summary:

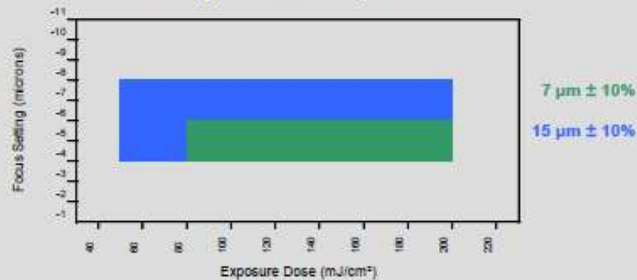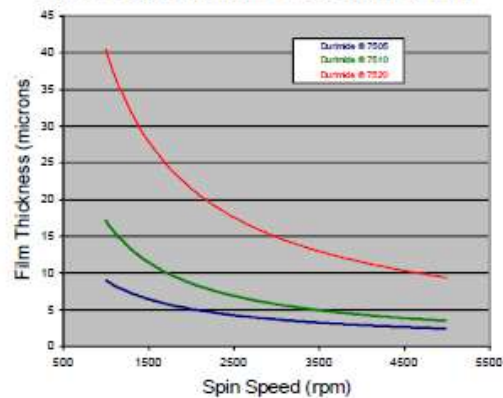|	
Substrate:	silicon
Soft Bake:	100°C /3mins
PIThickness:	10µm
Exposure Tool:	Canon g-line stepper .43NA
Post Exposure delay:	20-22°C/ 30 mins
Developer/Rinse:	HTRD2/RER600 30"/10"/15"

Process Window for a 7 & 15 µm CD space in a 12 µm film

7 µm ± 10%

15 µm ± 10%

Cured Film Thickness vs. Spin Speed

Durimide® 7500 undergoes a 45% shrinkage from softbake to cure.

References

1. Duffy, F. H., Burchfiel, J. L. and Lombroso, C. T. (1979), Brain electrical activity mapping (BEAM): A method for extending the clinical utility of EEG and evoked potential data. Ann Neurol., 5: 309-321.

2. D. Kim, C. Yeon, E. Chung and K. Kim, "A non-invasive flexible multi-channel electrode for in vivo mouse EEG recording," *SENSORS, 2014 IEEE*, Valencia, (2014)

3. Wasilczuk, A.Z., Proekt, A., Kelz, M.B., McKinstry-Wu, A.R. High-density Electroencephalographic Acquisition in a Rodent Model Using Low-cost and Open-source Resources. *J. Vis. Exp.* (117) (2016)

4. E. Niedermeyer, F. H. Lopes da Silva. Electroencephalography: Basic principles, clinical applications and related fields, 3rd edition (1993)

5. Jiahui Wang, Zhuolin Xiang, Gil Gerald Lasam Gammada, Nitish V. Thakora,b, Shih-Cheng Yen, Chengkuo Lee. Development of flexible multi-channel muscle interfaces with advanced sensing function, Sensors and Actuators, 249, (2016)

6. T Frederik Ceyssensa, Marta Bovet Carmonab, Dries Kila, Marjolijn Deprezc, Ester Tootend, Bart Nuttinc, Aya Takeokae, Detlef Balschunb, Michael Krafta, Robert Puersa; Chronic neural recording with probes of subcellular cross-section using 0.06 mm^2 dissolving microneedles as insertion device. Sensors and Actuators B: Chemicals 284, (2019)

7. Chung, J. E. et al. High-Density, Long-Lasting, and Multi-region Electrophysiological Recordings Using Polymer Electrode Arrays. *Neuron* 101, 21–31, (2019)

8. Richardson R Jr, Miller J, Reichert W (1993) Polyimides as biomaterials: preliminary biocompatibility testing. Biomaterials 14(8):627

9. Ghosh M, Mittal K (1996) Polyimides: fundamentals and applications. Marcel Dekker, New York, p 367

10. Natàlia de la Oliva, Xavier Navarro, Jaume del Valle "Time course study of long-term biocompatibility and foreign body reaction to intraneural polyimide-based implants" Journal of Biomedical Materials Research (2017)

11. Choi JH, Koch KP, Poppendieck W, Lee M, Shin HS. High resolution Electroencephalography in Freely Moving Mice. J Neurophysiol (2010).

12. Lee M, Shin HS, Choi JH. Simultaneous recording of brain activity and functional connectivity in the mouse brain. Conf Proc IEEE Eng Med Biol Soc. (2009)

13. D. Gupta, M. Islam, H. Nam, M. K. Lobo, F.-S. Choa, "Kapton polyimide-based EEG microelectrode array and interfaces for mice brainwave recordings and analysis" Proceedings of SPIE (2018)

14. Qinglei Meng, Deepa Gupta, Abenezer Wudenhe, Xiaoming Du, L. Elliot Hong, Fow-Sen Choa, "Three-dimensional EEG signal tracking for

reproducible monitoring of self-contemplating imagination", Adv. Sci. Technol. Eng. Syst. J. 2(3), 1634-1646 (2017);

15. Gupta D, Du X., Hong L., Choa F., "TMS-EEG based Source Localized Connectivity Signature Extraction by using Unsupervised Machine Learning", 9th International IEEE/EMBS Conference on Neural Engineering (NER), March 2019, Sam Francisco CA.

16. Kandel, Eric R., Schwartz, James H, Jessell, Thomas M., (2000), Principles of Neural Science, New York, McGraw-Hill, Health Professions Division, 2000.

17. Japan's National Institute for Basic Biology, www.nibb.ac.jp/brish/Gallery/cortexE.html

18. Comparative Mammalian Brain Collections
http://www.brainmuseum.org/index.html

19. Zhukov L, Weinstein D, Johnson CR, (2000), Independent Component Analysis for EEG Source Localization in Realistic Head Models. *Proceedings of the IEEE Engineering in Medicine and Biology Society, 22nd Annual International Conference*, **3**(19):87-96

20. St, Zschocke, E. J. Speckman, (1993) "Basic mechanisms of EEG", ISBN 978-1-4612-0341-4

21. Michel, C.M., & Murray, M.M. (2012). Towards the utilization of EEG as a brain imaging tool. *NeuroImage, 61*, 371-385.

22. Roth, G.D., & Dicke, U. (2005). Evolution of the brain and intelligence. *Trends in Cognitive Sciences, 9*, 250-257.

23. Piper, Diana & Schiecke, Karin & Leistritz, Lutz & Pester, Britta & Benninger, Franz & Feucht, Martha & Ungureanu, Georgeta & Strungaru, Rodica & Witte, Herbert. (2014). Synchronization analysis between heart rate variability and EEG activity before, during, and after epileptic seizure. Biomedizinische Technik. Biomedical engineering.

24. Hu, Xiangyou & Zhou, Xiangdong & He, Wanxia & Yang, Jun & Xiong, Wencheng & Wong, Philip & Wilson, Christopher & Yan, Riqiang. (2010). BACE1 Deficiency Causes Altered Neuronal Activity and Neurodegeneration. The Journal of Neuroscience. 30

25. Semple, B.D., Blomgren, K., Gimlin, K., Ferriero, D.M., & Noble-Haeusslein, L.J. (2013). Brain development in rodents and humans: Identifying benchmarks of maturation and vulnerability to injury across species. *Progress in Neurobiology, 106–107*, 1-16.

26. Watase, K., & Zoghbi, H.Y. (2003). Modelling brain diseases in mice: the challenges of design and analysis. *Nature Reviews Genetics, 4*, 296-307.

27. Parmentier, R., Ohtsu, H., Djebbara-Hannas, Z., Valatx, J., Watanabe, T., & Lin, J. (2002). Anatomical, physiological, and pharmacological characteristics of histidine decarboxylase knock-out mice: evidence for the role of brain histamine in behavioral and sleep-wake control. *The Journal of Neuroscience, 22 17*, 7695-711.

28. Neurotek Electrode: http://www.neurotek.ca/electrodes/ (screw electrode)

29. Vogler, E.C., Flynn, D.T., Busciglio, F., Bohannan, R.C., Tran, A., Mahavongtrakul, M., & Busciglio, J.A. (2017). Low Cost Electrode Assembly for EEG Recordings in Mice. *Front. Neurosci.*

30. Weltman, A., Yoo, J., & Meng, E. (2016). Flexible, Penetrating Brain Probes Enabled by Advances in Polymer Microfabrication. *Micromachines*.

31. Sawahata, H., Yamagiwa, S., Moriya, A., Dong, T., Oi, H., Ando, Y., Numano, R., Ishida, M., Koida, K., & Kawano, T. (2016). Single 5 μm diameter needle electrode block modules for unit recordings in vivo. *Scientific reports*.

32. Ungureanu, M., Bigan, C., Strungaru, R., and Lazarescu, V. (2004). Independent component analysis applied in biomedical signal processing. *Meas. Sci. Rev.* 4, 1–8

33. Brodbeck, V., Spinelli, L., Lascano, A.M., Pollo, C., Schaller, K., Vargas, M.I., Wissmeyer, M.P., Michel, C.M., & Seeck, M. (2010). Electrical source imaging for presurgical focus localization in epilepsy patients with normal MRI. *Epilepsia, 51 4*, 583-91.

34. Ji, Bowen & Guo, Zhejun & Wang, Minghao & Yang, Bin & Wang, Xiaolin & Li, Wen & Liu, Jingquan. (2018). Flexible polyimide-based hybrid opto-electric neural interface with 16 channels of micro-LEDs and electrodes. Microsystems & Nanoengineering.

35. AutoCAD website: https://www.autodesk.com/products/autocad/overview

36. Sun, Y., Lacour, S. P., Brooks, R. A., Rushton, N. , Fawcett, J. and Cameron, R. E. (2009), Assessment of the biocompatibility of photosensitive polyimide for implantable medical device use. J. Biomed. Mater. Res., 90A: 648-655.

37. Rubehn, B., & Stieglitz, T. (2010). In vitro evaluation of the long-term stability of polyimide as a material for neural implants. *Biomaterials, 31 13*, 3449-58 .

38. Ortigoza-Diaz, J., Scholten, K., Larson, C., Cobo, A., Hudson, T., Yoo, J., Baldwin, A., Hirschberg, A.W., & Meng, E. (2018). Techniques and Considerations in the Microfabrication of Parylene C Microelectromechanical Systems. *Micromachines*.

39. Seymour, J.P., & Kipke, D.R. (2007). Neural probe design for reduced tissue encapsulation in CNS. *Biomaterials, 28 25*, 3594-607.

40. Kotzar, G., Freas, M.S., Abel, P.B., Fleischman, A.J., Roy, S., Zorman, C., Moran, J.M., & Melzak, J. (2002). Evaluation of MEMS materials of construction for implantable medical devices. *Biomaterials, 23 13*, 2737-50 .

41. Kato, Y.X., Furukawa, S., Samejima, K., Hironaka, N., & Kashino, M. (2012). Photosensitive-polyimide based method for fabricating various neural electrode architectures. *Front. Neuroeng*.

42. MSDS Datasheet SU-8: www.microchem.com/pdf/SU-8-table-of-properties.pdf; www.microchem.com/pdf/SU-82000DataSheet2100and2150Ver5.pdf). MSDS Datasheet for Duramide: www.fujifilmusa.com/shared/bin/Durimide%207500_US12.pdf

43. Xiaoming Li, Lu Wang, Yubo Fan, Qingling Feng, and Fu-zhai Cui. (2012). Biocompatibility and toxicity of nanoparticles and nanotubes. J. Nanomaterials, 6.

44. Rodger, D., Fong, A.J., Li, W., Ameri, H., Ahuja, A.K., Gutierrez, C., Lavrov, I.A., Zhong, H., Menon, P.R., Meng, E., Burdick, J.W., Roy, R.R., Edgerton, V.R., Weiland, J.D., Humayun, M.S., & Tai, Y. (2008). Flexible parylene-based multielectrode array technology for high-density neural stimulation and recording, Sensors and Actuators, 449-460.

45. AZ5214 Recipe: www.tudelft.nl/en/faculty-of-applied-sciences/about-faculty/departments/quantum-nanoscience/kavli-nanolab-delft/equipment/process-recipes/resist-recipes/recipe-for-az5214-resist-in-positive-mode-lithography/

46. J. Monk, David & S. Soane, David & T. Howe, Roger. (1994). Hydrofluoric Acid Etching of Silicon Dioxide Sacrificial Layers II. Modeling. Journal of the Electrochemical Society. 141. 270-274